J. Condensed Matter Nucl. Sci. 34 (2021) 59–96

Research Article

Understanding Low Energy Nuclear Reactions

Péter Kálmán* and Tamás Keszthelyi

Budapest University of Technology and Economics, Institute of Physics, Budafoki út 8. F., H-1521 Budapest, Hungary

David J. Nagel

The George Washington University, 725 23rd Street NW, Washington DC 20052, USA

Abstract

This paper reviews a theoretical program to understand the field of low energy nuclear reactions (LENR), initially called cold fusion, which was a puzzle of the last three decades. A series of concepts, which were raised and partly elaborated, are presented. The key concept is a three-body mechanism, where one of the nuclei serves as a catalyst for the reaction of the other two. In these reactions, a single fusion product or two outgoing nuclei are created, along with the recoiled catalytic nucleus. They carry off the nuclear energy released, and heat the surrounding materials by multiple collisions. Importantly, they produce high energy γ radiation with negligible probability. So, this three-body idea solves the two major riddles of LENR, that nuclear reactions can occur at ordinary temperatures and without emitting γ radiation. Cross sections and rates are calculated using standard quantum mechanics, and accepted nuclear and solid-state physics. Their dependence on relevant densities, and on the reacting and catalytic nuclei, are explicit. The theoretical ideas and the results of their elaboration are compared with diverse data from LENR experiments with considerable success.

Keywords: Nuclear reactions: Specific reactions: General; Quantum mechanics; Fusion reactions

1. Introduction

It was reported 31 years ago that excess heat [1] and unexpected neutrons [2] appeared during electrolysis experiments with deuterized palladium hydrides. The experimental results were interpreted as evidence of nuclear fusion. After a short period of heated debate, skepticism overcame the scientific community. The failure to find the reported neutrons by others [3], and the published negative theoretical results [4–8], questioned even the credibility of the first reported results. However, in spite of the prevailing negative attitude of most nuclear physicists, authorities like Lamb [9] and Schwinger [10,11] asserted that cold fusion is theoretically possible. Researchers became divided on the possibility of cold fusion, a "schism" that remains. While mainstream physicists ignored the field [12], the research kept going during the last three decades. Great numbers of papers were published in the field, which is today called low-energy

*Corresponding author. E-mail: kalmanpeter3@gmail.com.

© 2020 ISCMNS. All rights reserved. ISSN 2227-3123

nuclear reactions, LENR. However, it seems obvious that the experiments carried out so far are not sufficiently clear to give precise information on the essential features of LENR. A detailed overview of the 31 years history of LENR goes beyond the scope of this paper. However, for summaries of laboratory results, see [13–18].

Our theoretical research program (Kálmán and Keszthelyi) over the past 17 years has been guided by the view that a theory which explains LENR must be consistent with physical knowledge. Theories, which explain some aspects of LENR but are in conflict with established parts of modern physics cannot be considered as satisfactory. The approaches of an early summary of attempts at theoretical explanations of LENR [19], and expectations of LENR theories discussed in [20], are consistent with this viewpoint.

The aim of writing this article was two-fold. One is to show to critical readers that it is possible to explain the phenomena of LENR within the framework of standard physics. It was also deemed useful to give guide lines to researchers in LENR. Some less successful initiatives, – along with possible mistakes committed, – are also discussed in order to spare unnecessary efforts by researchers in LENR. Remarks and notes by critics are also inserted in certain places, even if we do not agree with them, because they can be useful for the reader. The topic is very complex and delicate, so it must be stressed that we do not believe that all the problems related to LENR are solved.

Yet, in our opinion the fundamental question in LENR is to find a mechanism that helps nuclei of positive charge overcome the Coulomb barrier in order to react. In our quest for such a mechanism, it was recently pointed out in [21] KK that there is a close similarity between the forbidden optical transitions in quantum mechanics, and the way the cross section of nuclear reactions goes to zero at low energies due to Coulomb repulsion. It was found that any additional perturbation can resolve this forbidding of nuclear reactions, i.e., the disappearance of the cross section with decreasing energy. It is necessary for the perturbation theory to be carried out at least up to the second order according to the rules of quantum mechanics. This fact strongly enlarges the number of potential nuclear reactions. The significance of applying higher order perturbation calculation in nuclear reactions is also substantiated by the fact that it enables the explanation of the phenomenon of "Anomalous Internal Pair Creation" [22].

Given all the empirical data on LENR, and the theoretical results of our program, it is a good time to systematically overview both the experimental results of LENR and their possible explanations. This paper reviews our road to finding mechanisms, which may be responsible for LENR. Our results are not presented in chronological order. The major coherent ideas are treated together in sequence, each building on the earlier others. Theoretical findings and experimental observations are connected in each section and at the end of the paper.

Section 2 is the theoretical starting point. It is followed in Section 3 by the presentation and discussion of two early results, solid state internal conversion and attraction due to phonon exchange. Section 4 deals with two mechanisms adopted from quantum optics. The first is boson induced fusion (BIF), which is a laser like effect, and the second is a new loss mechanism based on a degenerate parametric amplifier mechanism, both of which can occur in crystalline solids. Section 5 contains the most essential explanations of LENR. Here, forbidden nuclear reactions, the important role of recoil due to perturbing Coulomb field of the surroundings, and charged particle catalyzed nuclear processes accompanied by heat production with lack of γ radiation are discussed. As an example, the second order model of nuclear reactions modified by the surroundings is propounded. The important results due to an approximate solution of a 3-body problem within the nuclear range and its consequence, the catalysis of nuclear reactions due to impurities, are also presented. Cross sections, counting rate- and power-densities are given also in this former model. Section 6 includes discussion of resonance-like third and fourth order processes, and Section 7 contains the results obtained in the case of cooperative processes. In Section 8, the importance of plasma-like states is pointed out. Section 9 is a summary of theoretical results obtained over 17 years in relation to laboratory data on LENR from the past 31 years. Section 10 is a summary of the major results of this theoretical program.

2. Theoretical Starting Point

Our starting point is based on the two major and central experimental facts about LENR, namely nuclear transmutations [23], which is the strongest evidence for the existence of LENR, and production of heat of nuclear origin, which is also well established [24]. Both of these effects occur without the emission of energetic γ radiation, which usually accompanies nuclear reactions. Accepting the existence of the LENR phenomena, i.e., the fact that heavy particles of low kinetic energy may take part in nuclear reactions, one is faced with the basic problem of how the reacting particles may overcome the Coulomb repulsion that exists between them. By examining the Coulomb solution $\varphi_{\rm Cb}$ (see formulae II. B 40-41 on p. 448 of [25]), which is the wave function in the relative coordinate $\mathbf{r}$ of two particles moving in their repelling Coulomb field, one can see that the contact probability density $|\varphi_{\rm Cb}|^2$ at $\mathbf{r} = \mathbf{0}$ reads

$$|\varphi_{\rm Cb}(\mathbf{r} = \mathbf{0})|^2 = \frac{f_{jk}^2}{V} \tag{1}$$

with V the volume of normalization (which disappears from the results of calculations) and

$$f_{jk} = \left| {\rm e}^{-\pi\eta_{jk}/2}\Gamma(1 + i\eta_{jk}) \right| = \sqrt{\frac{2\pi\eta_{jk}}{\exp(2\pi\eta_{jk}) - 1}}, \tag{2}$$

where $\Gamma(z)$ denotes the Gamma function and

$$\eta_{jk} = z_j z_k \alpha_f \frac{a_{jk} m_0 c}{\hbar |\mathbf{k}|} = z_j z_k \alpha_f \sqrt{a_{jk} \frac{m_0 c^2}{2\varepsilon}} \tag{3}$$

is the Sommerfeld parameter. $\mathbf{k}$ is the wave number vector of particles j and k in their relative motion, and ε is their kinetic energy in the center of mass system. z_j and z_k are the charge numbers of particles of rest masses $m_j = A_j m_0$ with $m_0 c^2 = 931.494$ MeV the atomic energy unit.

$$a_{jk} = \frac{A_j A_k}{A_j + A_k} \tag{4}$$

is the reduced mass number of the two particles. Furthermore, α_f is the fine structure constant, $\hbar$ is the reduced Planck constant, and c is the velocity of light in vacuum.

In some nuclear calculations, e.g. in the calculation of the alpha decay rate, an approximate solution [26] (the so called WKB approximation) responsible for the motion in the relative coordinates of the particles is used which results at $\mathbf{r} = \mathbf{0}$

$$|\varphi_{WKB}(\mathbf{r} = \mathbf{0})|^2 = \frac{\exp(-G_W)}{V}, \tag{5}$$

where $\exp(-G_W)$ is the so called Gamow-factor and

$$G_W = \sqrt{\frac{8\mu}{\hbar^2}} \int_R^{b_W} {\rm d}r \sqrt{V(r) - \varepsilon}. \tag{6}$$

Here, e.g. in the case of a pd reaction (see the next section), $V(r)$ is the interaction potential between p and d, and μ is the reduced mass of the two particles. r is their separation distance, R is the radius of the nucleus of higher nucleon number and b_W is the other classical turning point.

With decreasing $|\mathbf{k}|$ and ε, the contact probability density (1) at $\mathbf{r} = \mathbf{0}$ also decreases. But, if an attracting potential well of depth U is also present, then, as a good approximation, the $\varepsilon \rightarrow \varepsilon + U$ substitution may be done in (3) [27]. This recognition led to the introduction of U as a kinetic energy shift parameter called the screening energy for explanation of the enhancement of deuteron-deuteron fusion cross sections at low beam energies as being due to electron screening [27,28]. However, electron screening seems to be insufficiently strong to compensate for the Coulomb repulsion and make possible nuclear reactions at low kinetic energy $\varepsilon \simeq k_{\mathrm{B}}T$ near room temperature, where k_{B} is the Boltzmann constant and T is the absolute temperature. Since Coulomb repulsion is inevitable, one must find other reasons for the occurrence of LENR.

Given the above, two ideas were explored: (a) other effects caused by electrons and (b) some other mechanism, which produces a further attractive potential, in addition to the screened attractive Coulomb potential produced by electrons. These ideas must be considered in the context of the other problematic finding during LENR experiments, namely the absence of γ radiation.

3. Two Early Ideas

3.1. Solid state internal conversion

The absence of gamma radiation in LENR experiments, brings to the mind the internal conversion phenomenon, which has similar characteristics in atoms. In the usual internal conversion process the excitation energy of the nucleus is taken away by an atomic electron. The process takes place without γ emission [29,30]. In the simplest model of internal conversion process [29] the Coulomb interaction

$$V_{\mathrm{Cb}} = \sum_{i=1}^{Z} \frac{e^2}{|\mathbf{R} - \mathbf{r}_i|} \tag{7}$$

between the electron and the nucleus governs the decay. Here e is the elementary charge, Z is the proton number of the nucleus, $\mathbf{R}$ and $\mathbf{r}_i$ are the coordinates of the electron and the i-th proton, respectively. The Coulomb potential (7) is considered to be perturbation which causes the nuclear reaction and the transition probability per unit time of the process can be described in first order of perturbtion theory of quantum mechanics.

A similar reaction, the μ^- meson catalysed $p + d \rightarrow {}^3$He fusion reaction was investigated in 1957 [31] and the counting rate λ_{f} of the process was given in the form

$$\lambda_{\mathrm{f}} = A \left|\Phi_i\left(0\right)\right|^2, \tag{8}$$

where A is called nuclear reaction constant and $\Phi_{\mathrm{i}}\left(0\right)$ is the initial wave function of the p and d in their relative coordinate in the WKB approximation at zero separation, thus $\left|\Phi_{\mathrm{i}}\left(0\right)\right|^2 \sim \exp\left(-G_W\right)$ (see (6).

In [32] it was investigated how the $(e) + p + d \rightarrow (e') +^3$ He reaction can take place due to Coulomb interaction of an electron with a proton (p) and a deuteron (d). Here, the notation (e) refers to catalysis by an electron. (Our former terminology 'assistance' is changed in this work to 'catalysis' which expresses better the role of surrounding particles, both electrons and ions.) This analogue of atomic internal conversion reactions is called solid state internal conversion. In solid state internal conversion, most of the energy of the nuclear reaction (5.49 MeV) is taken away by the electron instead of the γ photon, which is emitted in the usual $p + d \rightarrow {}^3\mathrm{He}\,(5\ \mathrm{keV}) + \gamma\,(5.483\ \mathrm{MeV})$ nuclear fusion reaction. In the calculation [32], the Gamow-factor was used for the description of hindering due to the repelling Coulomb interaction between p and d. Thus, modification of the initial wavefunction in the nuclear range due to the Coulomb interaction with the electron was not considered. (It will be discussed in Section 5.)

Our result [32] obtained for the solid state internal conversion process [for the electron catalyzed reaction $(e) + p + d \rightarrow (e') + {}^3$He] was significantly larger than the result obtained in [6] for the case of hydrogen molecules. The solid state internal conversion calculation was repeated for the case of a lattice [33], where the initial catalyzing particles and one of the reacting particles were described by a Bloch-function [34]. The results of calculations based on the concept of solid state internal conversions indicated significant effects compared to molecular calculations. However, the obtained counting rates were not high enough and therefore they could not explain the reported extremely high dd fusion rates and excess heat [1]. Moreover, the solid state internal conversion mechanism would result in energetic electrons, the traces of which have been found in recent experiments [35] only.

3.2. Attraction due to phonon exchange

The other possibility, already noted, is the appearance of another new attractive potential, which is also present but not discovered yet. It was found [36] that optical phonon exchange can induce attraction between two deuterons in a d-filled Pd lattice. This attraction is similar to the attractive potential between electrons created by phonon exchange, which is known to be responsible for superconductivity [34]. The attraction due to optical phonon exchange seemed to be strong enough to be able to compensate partly for the Coulomb repulsion between deuterons leading to significant increase of the Gamow-factor. This mechanism is similar to the ones suggested by Schwinger in 1990 [11] and developed by Hagelstein from 2000 [37–39]. The idea was extended to the case of two different heavy particles, such as $p-d$, $^{7}\mathrm{Li}-p$ and $^{6}\mathrm{Li}-d$ [40].

The essence of our extended model is the following. The interaction potential of two different quasi-free particles of wave vector $\mathbf{k}_1$ and $\mathbf{k}_2$ due to phonon exchange in the λ^{th} branch in $\mathbf{K}$ space reads as [41]

$$V_{ph}\left(\mathbf{K},\lambda\right)=\left|g\left(\mathbf{K},\lambda\right)\right|^2\hbar\omega_{\mathbf{q},\lambda}\left(D_1\left(\mathbf{k}_1\right)+D_2\left(\mathbf{k}_2\right)\right), \tag{9}$$

where $\hbar\omega_{\mathbf{q},\lambda}$ is the energy of the optical phonon of wave number vector $\mathbf{q}$ in the first Brillouin zone and $\mathbf{K}=\mathbf{q}+\mathbf{G}$ outside the first Brillouin zone with $\mathbf{G}$ any vector of the reciprocal lattice. $g\left(\mathbf{K},\lambda\right)$ is the particle-phonon coupling function, as given in [36]. $\lambda=4,5,6$ for the optical branches, and

$$D_j\left(\mathbf{k}_j\right)=\frac{1}{\Delta E_j\left(\mathbf{k}_j,\mathbf{K}\right)^2-\left(\hbar\omega_{\mathbf{q},\lambda}\right)^2}, \tag{10}$$

for $j=1,2$ with $\Delta E_j\left(\mathbf{k}_j,\mathbf{K}\right)=E_j\left(\mathbf{k}_j\right)-E_j\left(\mathbf{k}_j+\mathbf{K}\right)$. Here, $E_j=\hbar^2\mathbf{k}_j^2/\left(2M_j\right)$ is the kinetic energy in the corresponding band and M_j is the rest mass of the particle. (For more details see [36] and [40].) It can be seen that the interaction is attractive if $\left|\Delta E_j\left(\mathbf{k}_j,\mathbf{K}\right)\right|<\hbar\omega_{\mathbf{q},\lambda}$. For heavier particles, because of their much larger rest mass, the inequality is fulfilled in a much larger volume of $\mathbf{K}$ space. Therefore, the attraction is expected to be much stronger than in the case of superconductivity of electrons.

It is worth mentioning that only a small fraction of hydrogenic isotopes dissolved in a Pd lattice may be supposed to be quasi-free. Moreover, the description of their movement in the intermediate quasi-free state by plane waves needs refinement [42].

If in (6) $b_W\gg R$ then the well known approximation [26] of G_W can be applied that gives

$$G_W=2\pi z_1 z_2\sqrt{\frac{\mu}{m_e}\frac{R_y}{\left|U_0(0)\right|}}. \tag{11}$$

Here μ is the reduced mass, z_1 and z_2 are the charge numbers of the reacting nuclei, R_y is the Rydberg energy and m_e is the rest mass of the electron. $U_0(0)$ is the value of the spherically symmetric part $U_O\left(r\right)$ of the attractive potential V_{ph} created by phonon exchange at $r=0$. (The validity of (11) is discussed on p. 787 of [36] and p. 298 of [40].)

The deuteron-density fraction $u=n_d/n_{\text{ion}}$, i.e. the deuteron number density n_d over metal ion number density n_{ion}, is an essential quantity of d filled metals. Numerical investigations resulted that $\left|U_0(0)\right|$ has significant u dependence, $\left|U_0(0)\right|$ increases with increasing u [36,40]. Consequently, the $G_W(u)$ function decreases with increasing u which causes a drastic increase of the Gamow-factor $\exp\left(-G_W\right)$ proportional to the rate. (The $U_O\left(r\right)$ and $V(r)=V_{\text{Coul}}+U_O(r)$ with V_{Coul} the Coulomb potential, were presented for some cases in [36] and [40] too). However, it was found that the attraction caused by phonon exchange is not strong enough by itself to compensate adequately the hindering effect of the repulsive Coulomb potential. Therefore, we searched for other mechanisms to explain enhanced deuterium fusion cross sections and low energy nuclear reactions.

4. Two Mechanisms from Quantum Optics

The anomalous x-ray transmission phenomenon [43,44] and the observation of fast-atom diffraction at surfaces [45,46] are well-established cases of the interactions of electromagnetic- and matter-waves with crystals. The production of bosons (^{4}He) in deuterated Pd during electrolysis inspired us to look at the possibility of the quantum optics of nuclei in crystalline solids [47,48].

4.1. Laser-like effect: boson induced fusion (BIF) in crystalline solids

Crystals, because of the Bragg law, can work like a resonator which selects the energy eigenstate

$$\Psi\left(\mathbf{r}\right)=\frac{1}{H}\sqrt{\frac{2}{d_j}}\exp(i\mathbf{k}_{\parallel j}\cdot\mathbf{r})\sin\left(\mathbf{k}_{\perp j}\cdot\mathbf{r}\right) \tag{12}$$

of the ^{4}He boson, which has nodal points on the crystal planes. That distribution makes absorption and scattering less probable when compared with the cosine-like case. Here, $\mathbf{r}$ denotes the coordinate of the ^{4}He particle, $\mathbf{k}_{\parallel j}$ and $\mathbf{k}_{\perp j}$ are the components of wave vector $\mathbf{k}_j=\mathbf{k}_{\parallel j}+\mathbf{k}_{\perp j}$ of ^{4}He parallel with and orthogonal to the j-th crystal plane, $\left(\mathbf{k}_{\parallel j}\cdot\mathbf{k}_{\perp j}=0\right)$. (The symbols $\parallel$ and $\perp$ refer to the components of any quantity parallel with and orthogonal to the j-th crystal plane.) With this notation, the Bragg law has the form $2\left|\mathbf{k}_{\perp j}\right|=n_{\mathrm{B}}\left|\mathbf{G}_j\right|$, where n_{B} is a positive integer, $\mathbf{G}_j$ is a reciprocal lattice vector with $\left|\mathbf{G}_j\right|=2\pi/d_j$, and d_j is the distance between the resonator planes [44]. An open resonator with length $H=d_j$ was assumed [47].

The nuclear fusion reaction

$$e+d_{\text{free}}+d_{\text{free}}\rightarrow\ {}^4\text{He}+e' \tag{13}$$

in a crystal resonator was considered by using results obtained earlier in the case of solid state internal conversion processes [32,33]. Since ^{4}He in (13) is a boson, induced emission can play an essential role in the reaction mechanism. Hence, we use the terminology of boson induced fusion (BIF) reactions. The possible BIF reactions may be identified by the participant particles. So, reaction (13) is called the electron catalyzed $\left(^4\text{He}\right)$ BIF reaction.

The component of the ^{4}He (bosonic) motion, which is orthogonal to the resonator planes and has energy eigenvalue $E_{\text{kin,He},\perp}(\mathbf{k}_{\perp j})=\hbar^2\mathbf{k}_{\perp j}^2/\left(2m_{\text{He}\,0}\right)$, is field quantized. The corresponding Hamiltonian is a type of oscillator with boson creation and annihilation operators ($a^+(\mathbf{k}_{\perp j})$ and $a(\mathbf{k}_{\perp j})$, respectively) in the mode with commutator $[a(\mathbf{k}_{\perp i}),a^+(\mathbf{k}_{\perp j})]=\delta_{ij}$. $m_{\text{He}\,0}c^2$ is the rest energy of ^{4}He. The part of the state of ^{4}He which describes the motion orthogonal to the resonator planes was described by number states $|n(\mathbf{k}_{\perp j})\rangle$.

The involved motions, namely the motion of the two deuterons, the electron, and ^{4}He parallel with the resonator planes, were treated quantum mechanically. Their initial (upper) state $|a\rangle$ of energy $E_a=2m_{d0}c^2+E_{\text{kin},1}+E_{\text{kin},2}+E_{e,i}$ is

$$|a\rangle=|d_1\rangle\otimes|d_2\rangle\otimes|e_{\mathrm{i}}\rangle\otimes|0\rangle. \tag{14}$$

$m_{d0}c^2$ denotes the rest energy of the deuteron, $E_{\text{kin},1}$, $E_{\text{kin},2}$ are the initial kinetic energies of the two deuterons of states $|d_1\rangle,|d_2\rangle$, respectively, and $E_{e,i}$ and $|e_{\mathrm{i}}\rangle$ are the kinetic energy and the initial state of the electron. The pumping mechanism, which prepares the ensemble of states $|a\rangle$, is thought to be injection of quasi-free deuterons by electrolysis or bombardment from hot gases or plasmas. The final (lower) state $|b\rangle$ of energy $E_b = m_{\text{He}\,0}c^2 + E_{\text{kin,He},\|} + E_{e,f}$ is

$$|b\rangle = |0\rangle \otimes |0\rangle \otimes |e_{\text{f}}\rangle \otimes |He_{\|}\rangle. \tag{15}$$

$E_{e,f} \simeq 23.77$ MeV and $|e_{\text{f}}\rangle$ are the kinetic energy and state of the electron in the final state, respectively. $E_{\text{kin,He},\|} = \hbar^2\mathbf{k}_{\|l}^2/\left(2m_{He0}\right) \simeq 75.7$ keV is the kinetic energy of ^{4} He of state $|\text{He}_{\|}\rangle$ with motion parallel with the resonator planes [47]. (The sum $E_{\text{kin,He},\|} + E_{e,f}$ has an uncertainty determined by the actual value of the sum $E_{\text{kin},1} + E_{\text{kin},2} + E_{e,i}$. Relativistic corrections which may be handled e.g. introducing off-mass-shell particles in variable mass theory of relativistic quantum mechanics [49–51] result $E_{\text{kin,He},\|} = 78.6$ keV, i.e. the error is 3.7%.) Thus the recoil by ^{4} He in the motion parallel with the resonator planes helps to fulfil momentum conservation of the electron-^{4} He system fulfilling the $\mathbf{k}_{\|l} = -\mathbf{k}_{ef}$ condition with $\mathbf{k}_{ef}$ the wave vector of the electron in the final state. The states $|b\rangle$ are degenerate states, as states $|e_{\text{f}}\rangle \otimes |\text{He}_{\|}\rangle$ of different directions of $\mathbf{k}_{ef}$ may have the same energy. This degeneracy was taken into account in the cross section calculation by summing up over all the possible final states. One pair of states $|a\rangle$ and $|b\rangle$ corresponds to a two-level system.

The interaction of an ensemble of the above two-level systems with the quantized boson field of state $|n(\mathbf{k}_{\perp j})\rangle$, which describes the perpendicular motion, can be treated in a way known in quantum optics [52]. The interaction Hamiltonian in the rotating wave approximation, which consists in discarding terms of frequency of approximately the double the basic frequency corresponding to the energy eigenvalue $E_{\text{kin,He},\perp}(\mathbf{k}_{\perp j})$, is

$$H_I = \sum_{\mathbf{k}_{\perp j},l}\left[V_{ab,jl}a^{+}(\mathbf{k}_{\perp j})\sigma_l + V_{ab,jl}^{*}a(\mathbf{k}_{\perp j})\sigma_l^{+}\right], \tag{16}$$

with $\sigma_l|a\rangle_l = |b\rangle_l$, and $\sigma_l^{+}|b\rangle_l = |a\rangle_l$. The suffix l relates to one definite $\mathbf{k}_{\|l} = -\mathbf{k}_{ef}$ situation.

The interaction Hamiltonian couples the l -th two-level system to the $\mathbf{k}_{\perp j}$ -th mode of the boson field, i.e., the direct product states $|A\rangle_l = |a\rangle_l \otimes |n(\mathbf{k}_{\perp j})\rangle$ and $|B\rangle_l = |b\rangle_l \otimes |n(\mathbf{k}_{\perp j})+1\rangle$ with a coupling constant $V_{ab,jl} \sim \exp\left(-G_W/2\right)$, where $\exp\left(-G_W\right)$ is the Gamow-factor and G_W is given by (11) with $z_1 = z_2 = 1$. G_W has u dependence through $U_0(0)$, which is the depth of the attractive interaction potential between two quasi-free deuterons induced by optical phonon exchange (see Fig. 3 of [40] and Fig. 5 of [36] and remember that $u = n_d/n_{ion}$ is the deuteron over metal ion number density.) The $\exp\left(-G_W\right)$ increases with the increase of the localized deuteron concentration (u) in Pd. Nuclear fusion due to the transition $|A\rangle_l \rightarrow |B\rangle_l$ happens as a consequence of the build-up of the boson field and thus, in appropriate conditions, the fusion rate may significantly increase due to induced emission in the laser-like process.

The coupling constant $V_{ab,jl}$ is calculated similarly to what was done in [32]

$$V_{ab,jl} = \int \varphi_{\text{i}}\left(\mathbf{r},\mathbf{R}\right)\chi_{\text{i}}\left(\mathbf{r}_3\right)\varphi_{f,jl}^{*}\left(\mathbf{r},\mathbf{R}\right)\chi_{\text{f}}^{*}\left(\mathbf{r}_3\right)\times \left(V_{\text{Cb}}[\mathbf{R}-\frac{1}{2}\mathbf{r}-\mathbf{r}_3] + V_{\text{Cb}}[\mathbf{R}+\frac{1}{2}\mathbf{r}-\mathbf{r}_3]\right)\mathrm{d}\mathbf{r}\,\mathrm{d}\mathbf{R}\,\mathrm{d}\mathbf{r}_3. \tag{17}$$

Here V_{Cb} is the Coulomb potential. $\mathbf{r} = \mathbf{r}_1 - \mathbf{r}_2$ and $\mathbf{R} = \mathbf{r}_1/2 + \mathbf{r}_2/2$ are the relative and the center of mass coordinates of the two deuterons of coordinates $\mathbf{r}_1$ and $\mathbf{r}_2$. $\mathbf{r}_3$ is the coordinate of the electron. The potential hole, which is created by the sum of Coulomb and optical phonon exchanged potentials (see e.g., Fig. 6. in [36]), was approximated by an oscillator-like potential. The initial two-deuteron state, which contains the essential $\exp\left(-G_W/2\right)$ factor, was determined as an oscillator-like state [53] of that potential. The initial and final electron states are plane waves.

The final state of ^{4}He is

$$\varphi_{f,jl}\left(\mathbf{r},\mathbf{R}\right) = \Phi_{\text{He}}\left(\mathbf{r}\right)\frac{\mathrm{e}^{i\mathbf{k}_{\|l}\cdot\mathbf{R}}}{H}\sqrt{\frac{2}{d_j}}\sin\left(\mathbf{k}_{\perp j}\cdot\mathbf{R}\right), \tag{18}$$

where $\Phi_{\text{He}}(\mathbf{r})$ is the $\mathbf{r}$ dependent part of the ^{4}He wave function. For the function Φ_{He}, we applied the Weisskopf approximation, i.e., $\Phi_{\text{He}} = \sqrt{3/(4\pi R_0^3)}$ if $r \leq R_0$ and $\Phi_{\text{He}} = 0$ if $r > R_0$ with R_0 the nuclear radius of ^{4}He.

Our aim was to estimate the threshold current during electrolysis, that is, the pumping mechanism of BIF. Therefore, the gain that determines the threshold number density $n_{a,th}$ of the number density n_a of the states $|a\rangle_l$ was determined by the threshold condition of the gain [54]. (For the further technical details, see [47]. A model, which is partly similar to the one discussed here, can be found in [38].) The numerical estimations were carried out using rather optimistic parameters since, connecting the problem to diffusion at the determination of threshold, partly quantum nature of the diffusion [55] was not taken into account.

It was recognized earlier that fast electrons are not found in LENR experiments of electrolysis type. This fact has led to the elaboration of a new loss mechanism, which may work in crystalline solids and is based on degenerate amplifier mechanism. It is discussed in the next subsection. Moreover, in view of later results (see V.B 'Roles of catalysis and recoil' below), it seems to be promising to re-examine the BIF problem with the Coulomb-recoil-type catalysis of an electron or a heavy particle instead of catalysis due to the attraction of phonon exchange. LENR observations of thermal instabilities [56], bursts, hot spots and crater-like damages [57–59] can be taken to indicate that BIF processes may sometimes occur. As already noted, the threshold observed in the current of electrolysis [14–16] may also be due to the laser like (non linear) mechanism. BIF is not restricted to the $dd \to {}^4$He reaction. The model may be extended to every nuclear reaction in which nucleus of integer spin is created in the final state. Heavy particles of integer spin, which act as catalysts for nuclear reactions (see Section 5), may take part in BIF like processes. They include, for example, isotopes of Pd of even mass numbers.

4.2. New loss mechanism in crystalline solids based on degenerate parametric amplifier

Fast electrons created in reaction (13) and having 23.77 MeV energy were not observed. Their absence may be explained by the following loss mechanism [48].

Fast particles, the outgoing electron and the ^{4}He particle, of opposite wave vectors $\mathbf{k}_{ef} = -\mathbf{k}_{\parallel l}(\equiv -\mathbf{K}_{\parallel})$, which occur in the final state of electron catalyzed BIF, are able to change the occupation numbers of the quantized motion of ^{4}He of BIF by two in a second order Coulomb scattering process with each other [48]. In this situation, the emission (or the absorption) of two quanta takes place in one step, while the wave vectors of the charged particles, the outgoing electron and the ^{4}He particle, are changed from $\mathbf{K}_{\parallel}, -\mathbf{K}_{\parallel}$ to $\mathbf{k}_{\parallel}, -\mathbf{k}_{\parallel}$. This special process can take place repeatedly if a reaction of BIF of type (13) is also possible. The whole process can be described by the interaction Hamiltonian (16) : $H_{I,New} = H_I + H_{I2}$ with

$$H_{I2} = \sum_{\mathbf{k}_{\perp j},l} \left[h_l^+(\mathbf{k}_{\perp j}) a^+(\mathbf{k}_{\perp j})^2 s_l^- + h_l^-(\mathbf{k}_{\perp j}) a(\mathbf{k}_{\perp j})^2 s_l^+ \right], \tag{19}$$

where s_l^- and s_l^+ are defined by the equations $s_l^- |a\rangle_l = 0$, $s_l^+ |a\rangle_l = 0$ and $s_l^- |b\rangle_l = |b'\rangle_{l'}$, $s_{l'}^+ |b'\rangle_{l'} = |b\rangle_l$, for $|a\rangle_l$ and $|b\rangle_l$ of the l-th two-level system (see (14) and (15)). The energy difference of states $|b\rangle_l$ and $|b'\rangle_{l'}$ is $E_{b,l} - E_{b',l'} = 2E_0$, where $E_0 = E_{\text{kin,He},\perp}(\mathbf{k}_{\perp j})$ is the energy of the quantized mode. The quantity $h_l^+(\mathbf{k}_{\perp j})$ can be calculated from the matrix element of the second order Coulomb scattering process of the electron and the ^{4}He particle on each other (as was described above), in which two quanta are emitted into the quantized mode.

On the other hand, as it is known from quantum optics [60] the Hamiltonian of form (19) describes the degenerate parametric amplification process which may be responsible for creating short laser pulses of huge intensities. Therfore (19) was reshaped into the form which is applied in quantum optics. The calculation results in $H_{I2} = i\hbar \frac{\chi}{2} \left[a^+(\mathbf{k}_{\perp j})^2 - a(\mathbf{k}_{\perp j})^2 \right]$ with $\chi = \chi_0 N_{\text{pair}}$, where N_{pair} is the instantaneous number of counter propagating $^4\text{He} - e$ pairs created. (χ_0 and other details can be found in [48].)

The initial state of the parametric amplification process is supplied by the laser-like BIF process [47], which creates the counter propagating $^4\mathrm{He}-e$ pairs. The parametric amplification process recreates the counter propagating $^4\mathrm{He}-e$ pairs, maintaining the possibility of parametric amplification process until one party of the pair scatters out from the repeatedly produced counter propagating state. Moreover, the ^{4}He mode of the parametric amplification process is the same as the ^{4}He mode of BIF. Thus the parametric amplification process reacts upon the BIF process, helping to increase the intensity of the quantized mode, and robustly amplifies the laser-like mode (the coherent state). The result is a very rapid increase of the rate of fusion. The coupling of BIF and parametric amplifier processes makes it difficult to give a thorough theoretical description of the whole process.

As a rough approximation, the degenerate parametric amplification process was treated separately from BIF. Like an initial state of the quantized motion of $^4\mathrm{He}_\perp$, that is built up in the BIF process, the coherent state $|\alpha_{^4\mathrm{He},\perp}\rangle$ with $\alpha_{^4\mathrm{He},\perp} = \alpha e^{i\Theta}$ was used. If the coherent state $|\alpha_{^4\mathrm{He},\perp}\rangle$ is perturbed with a Hamiltonian of type (19), then the mean value of its occupation number $\left\langle n_{^4\mathrm{He},\perp}(\mathbf{k}_{\perp j})\right\rangle$ evolves in time [60] as $\left\langle n_{^4\mathrm{He},\perp}(\mathbf{k}_{\perp j})\right\rangle = \alpha^2\left[\cosh(2\chi t)+\cos(2\Theta)\sinh(2\chi t)\right]+\sinh^2(\chi t)$.

It was shown in [48] that, in the above approximation, the process can take place during a time interval of order of magnitude of the very short life time of state $|b\rangle$ $\left(\tau_b \simeq 4\times10^{-18}\ s\ [47]\right)$. This leads to a huge pulse formation in the quantized mode during this time interval, which is accompanied with a very great number of successive boson creations. Thus, the loss mechanism described above may cause considerable decrease in the energy of fast charged particles created in BIF by converting a large part of the unquantized motion parallel with planes into the coherent motion perpendicular to lattice planes. (This mechanism may correspond to the loss term $\Gamma(E)$ introduced in the basic model of [39]) So, this mechanism might partially explain the discrepancies between the measured and expected energies of charged particles, especially fast electrons and their effects, as well as the conversion of nuclear energy into heat.

In [61] the constraints on energetic (especially α) particles in the Fleischmann–Pons experiment was studied and it was concluded ‘that only a small fraction of the reaction energy can be present in the alpha particle at the end of the reaction.’ It was also stated that, the alpha particle must be born with an energy less than 6.3–20.3 keV in order to be consistent with the absence of neutrons between 0.008 and 0.8 n/J as measured in Fleischmann–Pons experiments where excess heat is produced. These theoretical findings fit together well with the loss (dissipation) mechanism described above. The initial energy value of the created alpha particle is 75.7 keV which decreases abruptly (within $10^{-18}-10^{-17}$ s) into a small fraction of it in the degenerate amplifier mechanism. This indicates again that it is worth carrying out the coupled BIF and loss mechanism calculation with the aid of Coulomb recoil catalisation.

It is stated in [39] that the coupling between vibrations (optical phonon modes) and internal nuclear degrees of freedom is possible (mainly in deuterized metal systems, such as e.g. PdD). Furthermore, this theory is based on the generalization of the Dicke [62] and Jaynes-Cummings [63] models ([39] and references in it). In the case of optical phonons, it can produce a phenomenon, which is similar to superradiance, well known in quantum optics [64]. Further, the model is stated to be able to produce in itself valuable and promising results for explaining LENR observations.

However, the crystal resonator and our special loss mechanism based on it, are not applied in the above theory. One, who knows this theory, might think that there is no need to introduce a crystal resonator and the Coulomb-recoil-type catalysis at all. However, we are of the opinion that their (crystal resonator and Coulomb-recoil-type catalysis) action, which was proposed earlier, can significantly increase the effectiveness of conversion of nuclear energy to vibration (phonon modes).

5. Importance of Perturbation caused by Surroundings: the Three-body Mechanism

The mechanisms discussed above (solid state internal conversion, attraction due to phonon exchange, BIF and the loss mechanism) only produced partial understanding of LENR and can not explain satisfactorily the general phenomenon of nuclear transmutations. So, it became obvious that, if one wants to account for nuclear transmutations, a new basic mechanism must be found. That mechanism must considerably alter the contact probability density (1) due to the presence of the surroundings in order to explain LENR. Although it was shown only recently [21] that the effect of any perturbation provides the fundamental understanding of LENR, several studies were done in which this general statement was implicitly used, before full recognition of its importance. The concepts and results from these studies are reviewed in this section, along with our current understanding.

First, it was considered that if one of the reacting nuclei enters into solids, particularly into metals where free electrons are present, nuclei also interact with electrons by the usual Coulomb potential. That means the Hamiltonian governing the state of the nuclei must also contain the interaction Hamiltonian with the electrons [65]. It is a perturbation for the ingoing nucleus. The lowest order process, which must be taken into account, is a 2nd order process from the point of view of perturbation theory of quantum mechanics. Closely related to the study of 2nd order effects [65], the importance of the higher (3rd and 4th) order processes was also considered [66].

The electron-nucleus interaction led to electron catalyzed neutron exchange [67] and cooperative internal conversion [68] processes, as well. Those reactions are detailed below. They might be generalized by extending the Coulomb interaction to any charged particles of the surroundings. Such considerations lead to consideration of charged particle catalyzed nuclear reactions [69]. The investigations revealed that recoil [65] and, in particular the f_{jk}^2 factor (see (1) and (2)) have a crucial role for understanding LENR [70]. Recently, the investigation of the effect of impurities on nuclear reactions in plasma-like systems [71] led to the general understanding of forbidden nuclear reactions [21]. The discussion of these seemingly sporadic investigations is ordered systematically now.

5.1. Forbidden nuclear reactions

The cross section (σ) of nuclear reactions between charged particles j and k of charge numbers z_j and z_k has the form [72]

$$\sigma(\varepsilon) = S(\varepsilon)\exp\left[-2\pi\eta_{jk}(\varepsilon)\right]/\varepsilon, \tag{20}$$

where ε is the kinetic energy taken in the center of mass coordinate system, $S(\varepsilon)$ is the astrophysical factor and $\eta_{jk}(\varepsilon)$ is the Sommerfeld parameter. (We note that (20) is the definition of $S(\varepsilon)$ which can be determined from the measured cross section $\sigma(\varepsilon)$ with the aid of (20). $S(\varepsilon)$ and $S(0)$ are generally used in astrophysics.) The $\lim_{\varepsilon\to 0}\sigma(\varepsilon) = 0$ feature of the cross section indicates a disappearing rate of nuclear reactions in the $\varepsilon \to 0$ limit. This is analogous to the case of forbidden optical transitions in atomic physics (such as the hydrogen $2s_{1/2} - 1s_{1/2}$ transition, which is a forbidden electric dipole transition [73]). Hence, cross sections which have the form of (20) describe what are called forbidden nuclear reactions [21]. The forbiddenness is connected to the disappearing contact probability density of the two charged particles due to the Coulomb repulsion between them. The repulsion is manifested in the disappearance of the Coulomb solution at $\mathbf{r} = \mathbf{0}$ in the $\varepsilon \to 0$ limit, as was discussed above. Following the path used for the case of forbidden optical transitions [73], processes, which are second or higher orders from the point of view of perturbation theory, illuminate the case of forbidden nuclear reactions [21,74]. This general statement further strengthens the results of all the processes discussed below.

5.2. Roles of catalysis and recoil

If one wants to describe the interaction of a nucleus with another nucleus, while taking into consideration the interaction of the two nuclei with their surroundings (e.g., within an electrolyte, hot gas, plasma or solid), then the strongest perturbation is the Coulomb interaction. It must be taken into account. The lowest order process is the 2nd order one, which appears in perturbation theory, the graph of which can be seen in Fig. 1. The basic idea of recoil can be

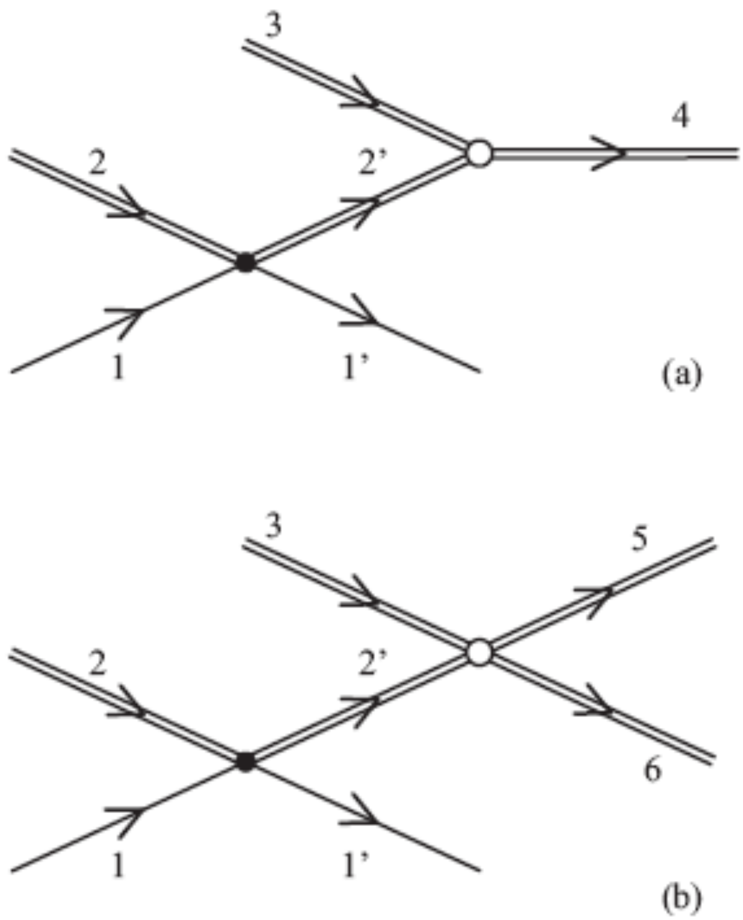

Figure 1. The graphs of Coulomb catalyzed nuclear reactions. The simple lines represent the initial (1) and final (1') states of the catalyzing particle. The doubled lines represent heavy, charged initial (2) particles (such as p, d), their intermediate state (2'), target nuclei (3) and reaction products (4, 5, 6). The filled dot denotes Coulomb-interaction and the open circle denotes nuclear (strong) interaction. Figure 1(a) is a capture (fusion) process and Fig. 1(b) is a reaction with two final fragments. Although the process in which particle 3 interacts first with particle 1 by Coulomb interaction is also possible, but the corresponding graphs are not drawn here.

demonstrated with the aid of Fig. 1(a), in which a Coulomb scattering is followed by a capture process governed by strong interaction.

As an example, let us consider the catalyzed $p + {}^{A_3}_{z_3}X \rightarrow {}^{A_4}_{z_4}Y$ reaction, especially the catalyzed $p + d \rightarrow {}^3_2$He model-process ($A_4 = A_3 + 1$, $z_4 = z_3 + 1$). It is thought that slow initial protons enter a solid (e.g., Pd) while quasi-free ${}^{A_3}_{z_3}X$ particles (e.g., deuterons) are also present within the Pd lattice. In this case, one of the slow protons (as particle 2 in Fig. 1(a)) can experience Coulomb interaction with a lattice constituent (Pd atom) of the solid (as particle 1), knocking out it from the lattice before reacting with an ${}^{A_3}_{z_3}X$ particle (e.g., a deuteron). Coulomb interaction is followed by strong interaction, which induces the nuclear capture process. The energy Δ of the nuclear reaction is divided between the heavy constituent (Pd atom) and the heavy nuclear product ${}_{z_4}^{A_4}Y$ (e.g., ${}_2^3$He). (The terminology 'before' and 'followed' are used according to time ordering of perturbation theory of quantum mechanics [75]) This process is a second order process in terms of standard perturbation theory. The rest masses of the participants are: $m_1 = A_1 m_0, m_2 = m_0, m_3 = A_3 m_0$ (e.g., $m_3 = 2m_0$) and $m_4 = A_4 m_0$ (e.g., $m_4 = 3m_0$) corresponding to the lattice constituent, the proton, the other nucleus (e.g., deuteron) and the nuclear product ${}_{z_4}^{A_4}Y$ (e.g., ${}_2^3$He), respectively. The states of the lattice constituent, the proton, the other nucleus and the nuclear product must fulfill energy and momentum conservation in the initial and final states, i.e., $E_{\rm i} = E_{\rm f}$, $\mathbf{k}_{\rm i} = \mathbf{k}_{\rm f}$, where $E_{\rm i}$ and $E_{\rm f}$ are the total energies, and $\mathbf{k}_{\rm i}$ and $\mathbf{k}_{\rm f}$ are the total wave number vectors in the initial and final states, respectively. If initially (before the Coulomb interaction) protons and ${}_{z_3}^{A_3}X$ particles (e.g., deuterons) move relatively slowly, and the lattice constituent has only vibration energy of thermal origin, then $E_{\rm i} = 0$ and $\mathbf{k}_{\rm i} = 0$ can be assumed. Therefore, in the final state $\mathbf{k}_{1'} + \mathbf{k}_4 = 0$, where $\mathbf{k}_{1'}$ and $\mathbf{k}_4$ are the wave vectors of the lattice constituent, knocked out from the lattice, and the nuclear product resulting $\mathbf{k}_{1'} = -\mathbf{k}_4 (= \mathbf{k})$. From energy conservation, it follows that in the final state $E_{\rm kin,1} + E_{\rm kin,4} = \Delta$ namely $\hbar^2\mathbf{k}^2/(2m_1) + \hbar^2\mathbf{k}^2/(2m_4) = \Delta$, which determines $\hbar\left|\mathbf{k}\right| = \hbar k = \sqrt{2m_0 a_{14}\Delta}$ with Δ the nuclear reaction energy (a_{14} is determined by (4)). (If $m_1 > m_4$ then the nuclear product (particle 4) will take away the larger part of Δ .) If the Coulomb interaction preserves the momentum (as was the case in the models used), then the Coulomb scattered proton (particle 2') also has wave vector $\mathbf{k}_{2'} = \mathbf{k}_4 = -\mathbf{k}$. That means its energy is $E_{2'} = \frac{\hbar^2 k^2}{2m_2} = a_{14}\Delta/A_2$ in the intermediate state (e.g. $E_{2'} = \frac{3A_1}{A_1+3}\Delta$ in the case of $p + d \to {}_2^3$He reaction. A_1 is the nucleon number of the heavy constituent (Pd atom) and $A_2 = 1$ in the case of proton capture discussed.)

For calculating nuclear matrix element (see Fig. 1(a)), the $f_{2'3}^2$ factor comes in via $\left|\varphi_{\rm Cb}\left(\mathbf{r}=\mathbf{0}\right)\right|^2$ (see (1)), which must be calculated in the center of mass (c.m.) system of particles 2' and 3. $E_{2'}(lab) = a_{14}\Delta/A_2$ is valid in the laboratory frame of reference (lab), the reference frame where the kinetic energy of the initial particles is negligible. Thus,

$$E_{2'}(\text{c.m.}) = \frac{m_3}{m_2+m_3}E_{2'}(\text{lab}) = \frac{A_3}{A_2\left(A_2+A_3\right)}a_{14}\Delta$$

must be substituted in (3), which gives

$$\eta_{2'3} = z_2 z_3 \alpha_{\rm f} A_2 \sqrt{\frac{m_0 c^2}{2a_{14}\Delta}} \tag{21}$$

Then, $\eta_{2'3} = z_3\alpha_{\rm f}\sqrt{m_0c^2/(2a_{14}\Delta)}$ with $z_2 = 1$ and $A_2 = 1$ corresponding to proton capture. In the case of the catalyzed $p + d \to {}_2^3$He reaction, $\Delta = 5.493$ MeV [76], which is the reaction energy. If $A_1 = 106$ corresponding to one of the Pd isotopes, then $2a_{14}\Delta = 32.05$ MeV, $\eta_{2'3} = 0.039$ and $f_{2'3}^2 = 0.88$. This must be compared to $f_{23}^2 = 1.06\times10^{-348}$ obtained with $\varepsilon = 1$ eV (producing $2\pi\eta_{23} = 807.9$) in the case of the usual $p + d \to {}_2^3\text{He} + \gamma$ reaction.

Moreover, in a proton capture process with particle 3 of mass number A_3 , the mass number of particle 4 becomes $A_4 = A_3 + 1$ and the reduced mass number $a_{14} = A_1\left(A_3+1\right)/\left(A_1+A_3+1\right)$. If $A_1 \simeq A_3 = \widehat{A}$, then $a_{14} = \widehat{A}/2$ and $2a_{14}\Delta = \widehat{A}\Delta = 572\ MeV$ at $\widehat{A} = 100$ with a typical (averaged) value of $\Delta = 5.72\ MeV$ (see Table I. of [70]). If $z_3 = 46$ then $\eta_{2'3} = 0.428$ and $f_{2'3}^2 = 0.196$. In this case, f_{23}^2 of usual p capture process is much smaller than the one obtained above ($f_{23}^2 = 1.06\times10^{-348}$) in the case of $p + d \to {}_2^3\text{He} + \gamma$ reaction.

Thus, the Coulomb scattered proton will have virtual momentum (and kinetic energy) in the intermediate state, which is large enough to make a drastic increase of the factor $f_{2'3}^2$, as illustrated in the two numerical examples above. In summary, the state of an incoming heavy, charged particle may be changed by a nucleus of the environment in such a way that (a) must not be neglected in rate calculations of nuclear processes and (b) makes possible dramatic increases in the probability of nuclear reactions. The nucleus of the environment, Pd in the illustration above, acts like a catalyst in enabling the nuclear reaction without participating in it.

5.3. Charged particle catalyzed nuclear processes: heat production and lack of γ radiation

As a consequence of the perturbations by atoms in the surroundings, two types of processes, which are called catalyzed processes, may become possible. The first

$$ {}_{z_1}^{A_1}V + {}_{z_2}^{A_2}w + {}_{z_3}^{A_3}X \rightarrow {}_{z_1}^{A_1}V' + {}_{z_3+z_2}^{A_3+A_2}Y + \Delta \quad (22) $$

is a capture of particle ${}_{z_2}^{A_2}w$ (e.g., proton (p) , deuteron (d), triton (t), ^{3}He, ^{4}He, etc.) catalyzed by ${}_{z_1}^{A_1}V$ (and ${}_{z_1}^{A_1}V'$). The second

$$ {}_{z_1}^{A_1}V + {}_{z_2}^{A_2}w + {}_{z_3}^{A_3}X \rightarrow {}_{z_1}^{A_1}V' + {}_{z_4}^{A_4}Y + {}_{z_5}^{A_5}W + \Delta \quad (23) $$

is a reaction with two final fragments ($A_2 + A_3 = A_4 + A_5$ and $z_2 + z_3 = z_4 + z_5$). The reaction energy Δ is the difference between the sum of the initial and final rest masses, that can be expressed with the aid of mass excesses as $\Delta = \Delta_{A_2,z_2} + \Delta_{A_3,z_3} - \Delta_{A_3+A_2,z_3+z_2}$ in case of (22), and $\Delta = \Delta_{A_2,z_2} + \Delta_{A_3,z_3} - \Delta_{A_4,z_4} - \Delta_{A_5,z_5}$ in case of (23), where Δ_{A_j,z_j} and $\Delta_{A_3+A_2,z_3+z_2}$ are the corresponding mass excesses [76]. The rest mass of particle 1 does not change since it only catalyzes the nuclear reaction. In case of catalysis by an electron, ${}_{z_1}^{A_1}V$ and ${}_{z_1}^{A_1}V'$ must be changed to e and e' in (22) and (23).

Usually, capture of particle ${}_{z_2}^{A_2}w$ may happen in the ${}_{z_2}^{A_2}w+ {}_{z_3}^{A_3}X \rightarrow {}_{z_3+z_2}^{A_3+A_2}Y + \gamma$ (with $\Delta > 0$) reaction, where γ emission is required by energy and momentum conservation. Accordingly, (22) describes a new type of ${}_{z_2}^{A_2}w$ -capture. In the usual ${}_{z_2}^{A_2}w$ -capture reaction, particles ${}_{z_3+z_2}^{A_3+A_2}Y$ and the γ take away the reaction energy, and the reaction is governed by the electromagnetic interaction. In reaction (22), the reaction energy is taken away by particles ${}_{z_1}^{A_1}V'$ and ${}_{z_3+z_2}^{A_3+A_2}Y$, while the reaction is governed by Coulomb as well as strong interactions. Importantly, the γ emission is missing.

It is essential to speak about what can be measured. In (22) and (23), the reaction energy is taken away by particles ${}_{z_1}^{A_1}V'$, ${}_{z_3+z_2}^{A_3+A_2}Y$ and ${}_{z_1}^{A_1}V'$, ${}_{z_4}^{A_4}Y$, ${}_{z_5}^{A_5}W$, respectively, as their kinetic energy. Since the catalyzing particle and the reaction product(s) are heavy (except the case of electron catalysis) and charged, they lose their energy in a very short distance through multiple collisions with the surroundings, if the matter of the environment is dense [77]. So, they convert the reaction energy efficiently into heat. Direct observation of the kinetic reaction products is difficult because they rapidly lose energy to and heat the lattice. That means the usual detection methods for products of nuclear reactions are generally not applicable. However, we note that some reaction particles occasionally escape and are measured by the use of CR-39, a solid state nuclear track detector [78,79].

The three-body interaction reviewed above explains the two main empirical observations of LENR, their occurrence and the absence of energetic radiation. It also shows that both protons and deuterons can experience LENR. And, as will be discussed more below, diverse nuclei can serve as catalysts for the reactions of light and other nuclei. We will show that heavy nuclei can also experience low energy nuclear reactions with light nuclei.

5.4. Second order model of nuclear reactions modified by a solid state environment

The change of state of heavy charged particles induced by solid state environments was modelled first in the following way [65]. Let us take two independent systems A and B, where A is a solid and B is an ensemble of free, heavy charged particles (e.g., free deuterons or protons entering the solid). The corresponding Hamiltonians are H_A and H_B. It is supposed that their eigenvalue problems are solved, and the complete set of the eigenvectors of the two independent systems are known. Let us extend the state vectors of systems A and B to the nuclear bound states, which are initially empty, under the assumption that the two systems do not interact at the beginning. The interaction between them, which is to be switched on adiabatically is described by the interaction Hamiltonian $V_{AB} = V_{\text{Cb}}(\mathbf{x}_{AB}) + V_{\text{st}}(\mathbf{x}_{AB})$, where V_{Cb} and V_{st} stand for the Coulomb and the strong interaction potentials, respectively. The suffixes A and B in their argument symbolize that one party of the interaction comes from system A and the other from system B.

In the process investigated, first a heavy, charged particle of system B takes part in a Coulomb scattering with any charged particle of system A. That interaction is followed by a strong interaction with some nucleus of system A, which leads to their final bound states. The graphs of the process can be seen in Fig. 1. The process of Fig. 1(a) is a nuclear capture process and the process of Fig. 1(b) is a nuclear reaction. (The processes, where the nuclear interaction is followed by the Coulomb interaction, can be neglected since the contact probability density (1) disappears in the $\varepsilon \to 0$ limit investigated.) Particles 1 and 3, belonging to system A are: electrons (e.g., free electrons in the case of a metal) or nuclei of the atoms forming the crystal and localized heavy, charged particles (bound, localized and quasi-free p, d and other nuclei) as nuclear targets. Particle 2 belongs to system B, that is a charged, heavy particle (e.g., proton (p) or deuteron (d)), which is supposed to move freely in a solid (e.g., in a metal). Since the aim was to show the fundamentals of the main effect, the core problem in LENR, the simplest description was chosen. That there may be identical, indistinguishable particles in systems A and B, and the dynamic evolution of the number N_2 of particles 2 of system B, were not investigated.

According to the rules of perturbation theory [74], the transition probability per unit time $\left(W_{fi}^{(2)}\right)$ of the capture process (see Fig. 1(a)) can be written as [21]

$$W_{\text{fi}}^{(2)} = \frac{2\pi}{\hbar} \int\int \left|T_{\text{fi}}^{(2)}\right|^2 \delta(E_{\text{f}} - \Delta) \frac{V^2}{(2\pi)^6} \mathrm{d}\mathbf{k}_{1'}\, \mathrm{d}\mathbf{k}_4 \tag{24}$$

with

$$T_{\text{fi}}^{(2)} = \int\int \sum_{s=2,3} \frac{V_{\text{st, f}\nu} V_{\text{Cb}}(1,s)_{\nu\text{i}}}{E_\nu - E_{\text{i}}} \frac{V^2}{(2\pi)^6}\, \mathrm{d}\mathbf{K}\, \mathrm{d}\mathbf{k}, \tag{25}$$

where E_{i}, E_ν and E_{f} are the kinetic energies in the initial, intermediate and final states, respectively, Δ is the reaction energy, i.e., the difference between the rest energies of the initial and final states, V is the volume of normalization. $V_{\text{Cb}}(1,s)_{\nu\text{i}}$, $s = 2,3$ is the matrix element of the Coulomb potential between the initial and intermediate states and $V_{\text{st, f}\nu}$ is the matrix element of the potential of the strong interaction between intermediate and final states. The intermediate states of particles 2 and 3 are determined by the wave number vectors $\mathbf{K}$ and $\mathbf{k}$ of their center of mass and relative motions, respectively.

$$E_{\text{f}} = E_{1'} + E_4, \tag{26}$$

$$E_\nu = E_{1'}(\mathbf{k}_{1'}) + E_{2'}(\mathbf{k}_{2'}), \tag{27}$$

where $E_{1'}$ is the kinetic energy and $\mathbf{k}_{1'}$ is the wave vector of the catalyzing particle 1' in the final state. $E_j(\mathbf{k}_j) = \hbar^2 k_j^2/(2m_j)$ is the kinetic energy of the j -th particle in the intermediate (particles1' and 2') and final (particles 1' and 4) states. If particle 1 is an electron [65] then

$$E_{1'} = \sqrt{(\hbar c)^2 k_{1'}^2 + m_e^2 c^4} - m_e c^2 \tag{28}$$

with $m_e c^2$ denoting the rest energy of the electron.

For the Coulomb potential we use its screened form

$$V_{\text{Cb}}(\mathbf{x}) = \frac{e^2 z_j z_k}{2\pi^2} \int \frac{1}{q^2 + q_{sc,jk}^2} \exp(i\mathbf{q} \cdot \mathbf{x}) \, \mathrm{d}\mathbf{q} \tag{29}$$

with $e^2 = \alpha_{\mathrm{f}} \hbar c$ and $q_{sc,jk}$ the screening parameter in the case of particles j and k. For the strong interaction we adopted in [65] the interaction potential

$$V_{st}(\mathbf{r}) = -2f^2 \frac{\exp(-s|\mathbf{r}|)}{|\mathbf{r}|}, \tag{30}$$

where the strong coupling strength $f^2 = 0.08\hbar c$ [80] and $1/s$ is the range of the strong interaction.

In [21] $V_{st}(2,3) = -V_0$ if $|\mathbf{r}| \leq b$ and $V_{st}(2,3) = 0$ if $|\mathbf{r}| > b$ with $\mathbf{r}$ the relative coordinate of particles 2 and 3. This form is used in the case of the reaction ${}^{A_1}_{z_1}V + p + d \rightarrow {}^{A_1}_{z_1}V' + {}^{3}_{2}\mathrm{He} + 5.493$ with $b = 2 \times 10^{-13}$ cm [21]. (For the calculation of catalyzed process with two final fragments, Fig. 1(b), see [21].)

The initial wavefunction $\psi_{1i}(\mathbf{r}_1)$ of particle 1, if it is heavy and localized, is given by [65]

$$\psi_{1i}(\mathbf{r}_1) = \left(\frac{\beta_1^2}{\pi}\right)^{3/4} \mathrm{e}^{-\frac{\beta_1^2}{2}\mathbf{r}_1^2} \tag{31}$$

or as a Bloch-function of the form [34]

$$\varphi_{\mathbf{k}_{1,i}}(\mathbf{r}_1) = N_1^{-1/2} \sum_{\mathbf{L}} \mathrm{e}^{i\mathbf{k}_{1,i} \cdot \mathbf{L}} a(\mathbf{r}_1 - \mathbf{L}) \tag{32}$$

with $\mathbf{r}_1$ the coordinate of particle 1. $\psi_{1i}(\mathbf{r}_1)$ is the wave function of the ground state of a 3-dimensional harmonic oscillator of angular frequency ω_1 with $\beta_1 = \sqrt{m_1\omega_1/\hbar}$ [53], where m_1 is the rest mass of particle 1. In the Bloch-function, $\mathbf{k}_{1,i}$ is wave number vector of the first Brillouin zone (BZ) of the reciprocal lattice. $a(\mathbf{r}_1 - \mathbf{L})$ is the Wannier-function, which is independent of $\mathbf{k}_{1,i}$ within the BZ, and is well localized around lattice site $\mathbf{L}$. N_1 is the number of lattice points of the lattice of particles 1 [21].

It was found in the first calculation using this model [65] that, contrary to the commonly accepted opinion, nuclear reactions in a solid metal environment can happen between heavy, charged particles of like (positive) charge of low initial energy. It was found that the electron catalyzed $d+d \rightarrow {}^4\mathrm{He}$ process has the largest rate among possible electron catalyzed dd processes. The first calculation of the total rates of the heavy charged particle catalyzed nuclear processes can also be found in [65].

In two subsequent papers, [69,70], the actual theoretical status of charge particle catalyzed reactions were summarized. Those papers contain the developments found up to 2015 and 2017. They included (a) the phenomenon of anomalous screening effect [27,28], (b) critical analysis of experiments of Fleischmann–Pons type, (c) possible charge particle catalyzed reactions in a Rossi-type reactor (E-cat) and (d) the possibility of nuclear transmutations due to charge particle catalyzed reactions.

5.5. Results due to an approximate solution of three-body problem in the nuclear range: catalysis by impurity nuclei

The connection between charge particle catalyzed reactions and LENR showed the importance of nuclear transmutation and recoil, as was emphasized in [70]. It was recognized that recoil by the catalyzing nucleus is the necessary condition for nuclear transmutations free of gamma radiation.

Inspired by this recognition, an approximate solution of the 3-body problem, which is valid in the nuclear range for two of the three particles that take part in the overall reaction, was constructed for the case of three free heavy charged particles, which interact via the screened Coulomb potential [21,71]. This model corresponds to the case when the environment consists of free particles, and can describe a gas of atoms, and plasmas.

The modification $\delta\varphi = \varphi - \varphi_{\mathrm{Cb}}$ of the wave function φ in relative coordinate $\mathbf{r}$ caused by the Coulomb interaction of particle 1 of coordinate $\mathbf{r}_1$ with the two other particles (particles 2 and 3 of coordinates $\mathbf{r}_2$ and $\mathbf{r}_3$) was determined in the $|\mathbf{r}| \lesssim R_2 + R_3$ range where $\mathbf{r} = \mathbf{r}_2 - \mathbf{r}_3$, R_2 and R_3 are nuclear radii of particles 2 and 3, and where the $\varphi_{\mathrm{Cb}}(\mathbf{r}) = 0$ approximation holds. It reads as

$$\delta\varphi\left(\mathbf{r}\right) = \sum_{s=2,3} \delta\varphi\left(s,\mathbf{r}\right) \tag{33}$$

where

$$\delta\varphi\left(s,\mathbf{r}\right) = z_1 z_s \alpha_{\mathrm{f}} \frac{4\pi\hbar c}{V^{5/2}} \frac{\mathrm{e}^{i(\mathbf{k_1 r_1} - \mathbf{k}_1 \mathbf{R})}}{\mathbf{k}_1^2 + q_{sc,1s}^2} \times \\ \times \frac{2m_0 a_{1s}}{\hbar^2 \mathbf{k}_1^2} \left[f_{23}\left(|\mathbf{k}|\right) \mathrm{e}^{i\mathbf{kr}} \right]_{\mathbf{k}=a(s)\mathbf{k}_1}. \tag{34}$$

Here, $\mathbf{k}_1$ is the wave number vector of particle 1 and $\mathbf{k}$ is the wave number vector of particles 2 and 3 in their relative motion. f_{23} comes from the Coulomb solution [25] and has the form given by (2). Finally, $a(s) = \left(-A_3\delta_{s,2} + A_2\delta_{s,3}\right) / \left(A_2 + A_3\right)$ and $s = 2,3$.

If the wavefunction does not vanish in the nuclear range, then nuclear processes are allowed to take place. That can be seen from the arguments $|\mathbf{k}| = |a(s)\mathbf{k}_1|$ of $f_{23}\left(|\mathbf{k}|\right)$ that are

$$\frac{A_3}{A_2 + A_3} k_1 \quad \text{and} \quad \frac{A_2}{A_2 + A_3} k_1$$

with $s = 2,3$, respectively, where $k_1 = |\mathbf{k}_1|$. In the case of a capture reaction, e.g., $\mathbf{k}_1^2 = 2m_0 a_{14} \Delta \hbar^{-2}$ where $\Delta\ (>0)$ is the energy of the reaction and A_4 in a_{14} is the mass number of the final nucleus in the capture reaction. ($f_{23}\left(|\mathbf{k}|\right)$ with $|\mathbf{k}| = \frac{A_3}{A_2+A_3} k_1$ is the same as the one given in subsection 'Roles of Catalysis and Recoil' with $\eta_{2'3}$ determined by (21).) Consequently, if particle 1 obtains large kinetic energy due to nuclear reaction, then the factors $f_{23}\left(|\mathbf{k}|\right)$ and the rate of the process will have considerable magnitude. In this case $\mathbf{k}_1^2 \gg q_{sc,1s}^2$ and one can neglect $q_{sc,jk}^2$ in the denominator of (34), i.e., the shielding of the Coulomb potential has no effect on the mechanisms discussed. Further numerical investigations of

$$f_{23}\left(|\mathbf{k}|\right) \quad \text{with} \quad |\mathbf{k}| = \frac{A_3}{A_2 + A_3} k_1 \quad \text{and} \quad |\mathbf{k}| = \frac{A_3}{A_2 + A_3} k_1$$

(the $s = 2,3$ cases, respectively, see above) show that nuclear reactions with proton (p), deuteron (d), triton (t), ^{3}He, ^{4}He, etc. may have increased transition probability per unit time.

Using this approximate 3-body solution in the case of nuclear fusion in a gas of atoms or a plasma, it was found that Coulomb scattering of fusionable nuclei on the screened Coulomb potential of the impurity nucleus, which only catalyzes the process, can diminish the hindering Coulomb repulsion between them and drastically increase the probability of nuclear fusion. Since the second order process does not demand the matter to be in ionized state, the catalysis of impurities can allow the plasma temperature required for nuclear reactions (such as fusion) to decrease significantly. The only requirement is that all components must be in atomic or ionic states. However, the quantitative results suggest that the density of the reactants and impurities must be considerably increased. The effective influence of wall-gas interaction, which was also discussed [21,71], brings up the possible importance of gas-metal surface processes. Promising new fuel mixes were also put forward. Based on these results, it may be expected that searches for new approaches to energy production by nuclear fusion are possible [71]. Impurity catalysis in an atomic or ionic gas, and their interactions with wall of the equipment, may be connected to LENR observations, which were reported in gas discharges [81].

5.6. Cross sections, counting rate- and power-densities

The transition probability per unit time of charged particle catalyzed processes can be determined in accordance with the rules of quantum mechanics (see e.g., (24)) [74]. Having the transition probability per unit time, the cross section can also be deduced in standard fashion. It was shown in [24,74] that the cross sections $\sigma_{23}^{(2)}$ of reactions (22) and (23) have the form

$$\sigma_{23}^{(2)} = \frac{n_1 S_{\prime\text{reaction}\prime}}{v_{23}}, \tag{35}$$

where n_1 is the number density of particle 1, and v_{23} is the relative velocity of particles 2 and 3. This is a general result. The $\sigma_{23}^{(2)} \sim 1/v_{23}$, similar to thermal neutron capture cross sections [29]. $S_{\prime\text{reaction}\prime}$ was determined in the case of the catalyzed $p + d \to {}^3$He reaction and the reaction family (23) in [21,71]. In the case of (23) $S_{\prime\text{reaction}\prime}$ was deduced from the astrophysical factor $S(0)$ (see (20) and [72]) at $\varepsilon = 0$. $S_{\prime\text{reaction}\prime}$ is temperature independent and $S_{\prime\text{reaction}\prime} \sim z_1^2 S(0)$ [21].

As a numerical example, we take the $d(d,t)p$ reaction investigated in [28,82]. In [21], the cross section of the catalyzed, second order process $\sigma_{23}^{(2)}$ was compared to the cross section $\sigma_{23}^{(1)}$ of the usual reaction in a d filled Pd. For the cross sections $\sigma_{23}^{(2)} = n_1 S_{\text{d(d, t)p}}/v_{23} = 7.77 \times 10^{-11}/\sqrt{\varepsilon(\text{in MeV})}$ b with $n_1(\text{Pd}) = 1.36 \times 10^{23}$ cm^{-3} and $\sigma_{23}^{(1)} = 0.0571 \exp(-0.990/\sqrt{\varepsilon(\text{in MeV})})/\varepsilon(\text{ in MeV})$ b were obtained. If $\sigma_{23}^{(2)} > \sigma_{23}^{(1)}$, then the second order process dominates, which is the case if $\varepsilon < 0.001762$ MeV. This result fits well with the experimental data of [82]. Consequently, the anomalous screening phenomenon in the case of $d(d,t)p$ reaction may be connected to the Pd catalyzed process discussed here. Similar results were obtained in the case of electron catalyzed $d(d,t)p$ reaction [83].

The above numerical example shows that the cross section $\sigma_{23}^{(2)}$ of heavy particle catalyzed processes, which can become the dominant among the processes discussed here at appropriately high value of n_1, can become comparable with the very small cross section of the direct process if the number density n_1 of the catalyzing particle becomes large (e.g. 10^{23} cm^{-3}, see above). However, the reaction products, which are heavy charge particles, decelerate in a very short distance of about μm order of magnitude [77] which fact strongly hinders their observation (as is said in Section V.C too). This fact is the reason for most experimental problems of LENR, it obstructs direct, quantitative comparison of theoretical results with experimental data and it makes very difficult to carry out the recently proposed experiment of coincidence type [21].

The counting rate density ($r_{\prime\text{reaction}\prime}$) and power density ($p_{\prime\text{reaction}\prime}$) are

$$r_{\prime\text{reaction}\prime} = n_3 n_2 n_1 S_{\prime\text{reaction}\prime} \tag{36}$$

and

$$p_{\prime\text{reaction}\prime} = r_{\prime\text{reaction}\prime}\Delta = n_1 n_2 n_3 S_{\prime\text{reaction}\prime}\Delta, \tag{37}$$

where n_2 and n_3 are the number densities of particles 2 and 3. The counting rate- and power-densities are temperature independent. It was also shown that if one of the three particles comes from within a solid (metal) that contains atoms with nuclei of charge and mass numbers z_j and A_j then $n_j = N_{jc}/v_c$, where v_c is the volume of elementary cell of the solid and N_{jc} is the number of particles j in the elementary cell [21]. The model may also be applied if at least one of reacting particles is in a highly mobile, quasi-free state in or on solids, e.g., in the case of highly mobile, quasi-free protons and deuterons. Thus, the model is valid in the cases of electrolysis cells, gas-solid surfaces and gas discharges. Many numerical results for counting rate- and power-densities for 28 specific nuclear reactions can be found in [21] and [84]. ^{4}He was produced in 19 of the cases, which had two final fragments. In general, we have found many reactions for the production of ^{4}He by different mechanisms.

Some results of our $S_{\rm reaction}$ and counting rate density calculations can be found in Tables 1 and 2. The energies (spin$^{\rm parities}$) of the considered excited states are: ^{12}C, 4.439 MeV (2^+) ; ^{20}Ne, 1.634 MeV (2^+) and ^{23}Na, 0.4400 MeV $(5/2^+)$. $S(\varepsilon)$ is taken from [85], $S(0) = 3.5 \times 10^7$ MeVb and $S(0) = 100$ MeVb are taken from [72, 86], respectively. Note that the $S(0) = 1.0 \times 10^{16}$ MeVb [87] value seems to be an under-estimation of $S(0)$ [88].

It is worth mentioning, as further numerical examples, a few cases of power and counting rate densities. In an atomic or ionic environment, Xe catalyzed $d(t,n)^4_2$He and $^{11}_5$B$(p,\alpha)^8_4$Be reactions can produce power densities of 5570 W cm^{-3} and 13.2 W cm^{-3}, respectively, if the product $n_1 n_2 n_3 = 1.861 \times 10^{61}\ cm^{-9}$, which is the case, e.g., if $n_1 = n_2 = n_3 = 2.65 \times 10^{20}$ cm^{-3}. In similar circumstances, the $d(d,n)^3_2$He and $d(d,p)t$ reactions can produce 9.82 W cm^{-3} and 13.2 W cm^{-3}, respectively [21,71]. Moreover, the ^{58}Ni catalyzed ^{15}N$(p,\alpha)^{12}$C, ^{14}N$(^6$Li$,\alpha)^{16}$O, ^{14}N$(^7$Li$,\alpha)^{17}$O and ^{12}C$(^{12}$C$,\alpha)^{20}$Ne reactions have counting rate densities 1.61×10^{11} cm^{-3} s^{-1}, 9.64×10^{10} cm^{-3} s^{-1}, 1.90×10^{10} cm^{-3} s^{-1} , and 4390 cm^{-3} s^{-1}, respectively, with $n_1 n_2 n_3 = 1.861 \times 10^{61}$ cm^{-9} [84]. These results indicate that dd reactions have lost their unique role in LENR. They can be important both scientifically and practically. However, it is now clear that "cold fusion" is simply a sub-case of the much more general and numerous LENR.

The result (34) indicates that the most significant increase of the cross section caused by Coulomb interaction of reacting particles $(2$ and $3)$ with $^{A_1}_{z_1}V$ originates from factors f_{23} derived from the Coulomb solutions of particles $2,3$ of high ε. According to perturbation calculation [21] these Coulomb states are mixed to the state of $\varepsilon = 0$ and factors f_{23}, which come from these Coulomb solutions, are defined as

$$f^2_{23}(s,\Delta) = \frac{2\pi\eta_{23}(s,\Delta)}{\exp\left[2\pi\eta_{23}\left(s,\Delta\right)\right] - 1} \tag{38}$$

with

$$\eta_{23}\left(s,\Delta\right) = z_2 z_3 \alpha_{\rm f} \frac{a_{23}}{a(s)} \sqrt{\frac{m_0 c^2}{2 a_{14} \Delta}}, \tag{39}$$

where $a(s) = \left|-A_3 \delta_{s,2} + A_2 \delta_{s,3}\right| / \left(A_2 + A_3\right)$ with $s = 2,3$ and $a_{jk} = A_j A_k / \left(A_j + A_k\right)$ is the reduced mass number of particles j and k of mass numbers A_j and A_k. The cross section and the counting rate density are proportional to a sum of terms proportional to $f_{23}(s,\Delta) f_{23}(s',\Delta)$.

In the case of proton capture ($z_2 = 1$, $A_2 = 1$) the $s = 2$ case with $a(2) = A_3/\left(1 + A_3\right)$ gives the largest f_{23} value therefore only the leading $f^2_{23}(2,\Delta)$ will be studied on. (One should remember that $f^2_{23}(2,\Delta)$ must be compared to $\exp\left[-2\pi\eta_{23}\left(\varepsilon\right)\right]$ which comes from the cross section $\sigma\left(\varepsilon\right)$ of usual nuclear reactions between charged particles 2 and 3 of charge numbers z_2 and z_3 (see (20) and [72] where $\eta_{23}\left(\varepsilon\right)$ is the Sommerfeld parameter given by (3) and ε is the kinetic energy taken in the center of mass coordinate system. If $\varepsilon \to 0$ then $\sigma\left(\varepsilon\right)$ disappears.)

Capture reactions of type (22) will have cross section $\sigma^{(2)}_{23}$ of considerable magnitude if $\eta_{23} < 1$ (if $\eta_{23} = 1$ then $f^2_{23} = 0.012$). In the case of proton capture using $\eta_{23}(2,\Delta)$ the $\eta_{23} < 1$ leads to the condition

$$z_3 \lesssim \left[2 a_{14} \Delta / \left(\alpha^2_{\rm f} m_0 c^2\right)\right]^{1/2}. \tag{40}$$

In the case of heavy $1,3$ and 4 particles, $A_1 \simeq A_3 \simeq A_4$ and $a_{14} \simeq A_4/2 \gtrsim z_4 \simeq z_3$ one has

$$z_3 \lesssim 2\Delta / \left(\alpha^2_{\rm f} m_0 c^2\right) = 40.30 \times \Delta(\text{in MeV}). \tag{41}$$

For d -capture this condition modifies as

$$z_3 \lesssim \Delta / \left(2\alpha^2_{\rm f} m_0 c^2\right) = 10.08 \times \Delta(\text{in MeV}). \tag{42}$$

Table 1. S_{reaction}(in cm^6s^{-1}) and counting rate density r_{reaction}(in $\text{cm}^{-3}s^{-1}$) of Ni (of mass number 58) assisted reactions with two final fragments. Δ(in MeV) is the energy of the reaction. $S(0)$(in MeVb) is the astrophysical factor at $\varepsilon = 0$, where ε is the center of mass kinetic energy. $r_{\text{reaction}} = n_1 n_2 n_3 S_{\text{reaction}}$ is the counting rate density (called rate in astrophysics) that is calculated with $n_1 n_2 n_3 = 1.861 \times 10^{61}$ cm^{-9}. The subscripts 0 and 1 refer to ground and first excited final nuclear states. The energies (spin^{parities}) of the considered excited states are: ^{12}C, 4.439 MeV (2^+); ^{20}Ne, 1.634 MeV (2^+) and ^{23}Na, 0.4400 MeV$(5/2^+)$. $S(\varepsilon)$ is taken from [85], $S(0) = 3.5 \times 10^7$ MeVb, $S(0) = 100$ MeVb are taken from [72], [86], respectively. Furthermore, the $S(0) = 1.0 \times 10^{16}$ MeVb [87] value seems to be an under-estimation of $S(0)$ [88].

Reaction	S_{reaction}	Δ	r_{reaction}
$S(\varepsilon)$			
^{15} N(p, α_0)^{12} C	8.20×10^{-51}	4.965	1.61×10^{11}
^{15} N(p, α_1)^{12} C	1.63×10^{-51}	0.526	3.19×10^{10}
$S(0) = 100$			
^{23} Na(p, α_0)^{20} Ne	5.59×10^{-52}	2.377	1.10×10^{10}
^{23} Na(p, α_1)^{20} Ne	4.43×10^{-52}	0.743	8.68×10^{9}
$S(0) = 3.5 \times 10^7$			
^{14} N(^{7} Li, α_0)^{17} O	9.71×10^{-52}	16.155	1.90×10^{10}
^{14} N(^{6} Li, α_0)^{16} O	4.92×10^{-51}	19.262	9.64×10^{10}
^{16} O(^{7} Li, α_0)^{19} F	2.43×10^{-53}	9.233	4.76×10^{8}
^{16} O(^{6} Li, α_0)^{18} F	2.13×10^{-53}	6.051	4.18×10^{8}
^{17} O(α_0, n)^{20} Ne	3.46×10^{-54}	0.587	6.79×10^{7}
S(0)=1.0×10^{16}			
^{12} C(^{12} C, α_0)^{20} Ne	2.24×10^{-58}	4.617	4390
^{12} C(^{12} C, α_1)^{20} Ne	4.43×10^{-63}	2.983	0.087
^{12} C($^{12}C, p_0$)^{23} Na	8.11×10^{-67}	2.241	1.60×10^{-5}
^{12} C($^{12}C, p_1$)^{23} Na	4.39×10^{-70}	1.801	8.61×10^{-9}

All these mean that e.g. even the ^{238}U+ d+ ^{235}U $\rightarrow$ ^{238}U$'$+ ^{237}Np + 9.182 MeV d-capture reaction can happen with a non-negligible probability (counting rate density). As a result we are faced with plenty of possible p - and d-capture reactions of type (22). Obviously the $^{A_1}_{z_1}$V+ d+ $d \rightarrow$ $^{A_1}_{z_1}$V$'$+ ^{4}He + 23.845 MeV reaction may also happen. An essential consequence of the possibility of p - and d -capture reactions of type (22) is the possibility of nuclear transmutation of all the elements of the periodic table.

It was found that not only in the case of the earlier investigated reactions (the reactions from $d(d,n)^3$He up to $^{11}B(p,\alpha)^8$Be, see Table 1 of [21]) but in view of the results of reactions discussed here (reactions from ^{15}N$(p,\alpha_0)^{12}$C up to ^{12}C(^{12}C, α_1)^{20}Ne, see Table I here and the reactions of Table 2) the counting rate density of reaction can have considerable magnitude if the number densities n_j $(j = 1, 2, 3)$ of the initial particles reach appropriately high values.

6. Other Processes due to Coulomb Field of Surroundings: Resonance-Like third and fourth Order Processes

In [65,21,71,84], only processes of second order were discussed. In [66], the family of double nuclear processes, which has special interest from the point of view of LENR, were considered. The 3rd- and 4th-order double nuclear

Table 2. S_{reaction} (in cm^6 s^{-1}) and counting rate density r_{reaction} (in cm^{-3}s^{-1}) of Pt (of mass number 195) assisted reactions with two final fragments. Δ (in MeV) is the energy of the reaction. $r_{\text{reaction}} = n_1 n_2 n_3 S_{\text{reaction}}$ is the counting rate density (called rate in astrophysics) that is calculated with $n_1 n_2 n_3 = 1.861 \times 10^{61}$ cm^{-9}. $S(0)$ (in MeVb) is the astrophysical factor at $\varepsilon = 0$, where ε is the center of mass kinetic energy. $S(0) = 3.5 \times 10^7$ MeVb, $S(0) = 100$ MeVb are taken from [72], [86], respectively.

Reaction	S_{reaction}	Δ	r_{reaction}
S(0)=100			
^{16} O(d, α_0)^{14} N	1.86×10^{-51}	3.011	3.66×10^{10}
^{17} O(d, α_0)^{15} N	2.11×10^{-51}	9.800	4.15×10^{10}
^{18} O(d, α_0)^{16} N	1.96×10^{-51}	4.245	3.85×10^{10}
S(0)=3.5×10^7			
^{16} O(d, α_0)^{14} N	6.52×10^{-46}	3.011	1.28×10^{16}
^{17} O(d, α_0)^{15} N	7.40×10^{-46}	9.800	1.45×10^{16}
^{18} O(d, α_0)^{16} N	6.86×10^{-46}	4.245	1.35×10^{16}

processes were investigated, the graphs of which can be seen in Figs. 2 and 3. It must be emphasized at the outset that resonances may occur in both double nuclear processes. The reason for the possibility of resonance is that the continuum of the kinetic energy of an intermediate state is shifted down by the energy of the (first) nuclear transition, and therefore one of the denominators in the perturbation theory can be equal to zero. The occurrence of resonances increases the counting rate significantly. In this section, we discuss a few resonant processes.

6.1. Resonance-like heavy charged particle catalyzed double nuclear processes

First, the resonance-like heavy charged particle catalyzed double nuclear processes (see Fig. 2) are discussed. The particles in Fig. 2 are all heavy, and positively charged. The ingoing particle is particle 2, which belongs to system B (the ensemble of incoming particles constitutes system B). It was supposed that it has moderately low energy (of about keV order of magnitude, as in low-energy dd fusion experiments). Although in [66] it was supposed that particle 2 is created in the second order processes discussed in [65] or after it during the decelerating process, it was pointed out in [21] that it may have very low kinetic energy.

In the resonance-like process, particle 2 scatters by Coulomb interaction with particle 1 of initial state $\psi_{1i}(\mathbf{x})$ of the form (31). Particle 1 is localized in the solid (system A). Particles 3 and 4 are the nuclear targets of system A. The particles in the intermediate states 1' and 2' may pick up a large enough wave vector to overcome the Coulomb repulsion due to particles 3 and 4. Particles 5 and 6 are products of the process. The nuclear processes $1' + 4 \rightarrow 5$ and $2' + 3 \rightarrow 6$ can take place as the consequence of the Coulomb scattering of particles 1 and 2 on each other. Here, both nuclear processes are thought to be nuclear captures. With the aid of the graphs of Fig. 2 one can see that the processes

$$ {}^{A_2}_{z_2}\mathrm{w} + {}^{A_3}_{z_3}X \rightarrow {}^{A_2+A_3}_{z_2+z_3}Y + \Delta_{23} \tag{43} $$

and

$$ {}^{A_1}_{z_1}\mathrm{V} + {}^{A_4}_{z_4}\mathrm{v} \longrightarrow {}^{A_1+A_4}_{z_1+z_4}y + \Delta_{14} \tag{44} $$

are coupled to the

$$ {}^{A_1}_{z_1}\mathrm{V} + {}^{A_4}_{z_4}\mathrm{v} + {}^{A_2}_{z_2}\mathrm{w} + {}^{A_3}_{z_3}X \rightarrow {}^{A_2+A_3}_{z_2+z_3}\mathrm{Y} + {}^{A_1+A_4}_{z_1+z_4}\mathrm{y} + \Delta \tag{45} $$

double nuclear capture process due to Coulomb interaction of particles ${}^{A_1}_{z_1}\mathrm{V}$ and ${}^{A_2}_{z_2}\mathrm{w}$. Here $\Delta = \Delta_{23} + \Delta_{14}$ is the energy of the double reaction. Naturally, if the particles are all free, then Coulomb interactions between particles 2, 3 and 1, 4 must be taken into account too. Correspondingly, contributions due to Coulomb interaction of particles $(1, 3)$, $(2, 4)$ and $(3, 4)$ must also be considered in calculating $T^{(3)}_{\mathrm{fi}}$ [66]. It can be shown that the process may have resonance-like character [66], if the masses of particles 5 and 6 differ significantly. Therefore, when calculating the counting rate, it is enough to calculate the dominant contribution resulting from the leading graph, which is Fig. 2(a) in the case $m_5 \gg m_6$, discussed in [66].

Not only capture reactions may couple. Coupling may also happen between reactions with two final fragments, and between a capture reaction and a reaction with two final fragments, as well. Such reactions are not discussed here. Moreover, one can conclude that there may be a great variety of possible quasi-resonant heavy charged particle catalyzed double nuclear reactions.

6.2. Electron catalyzed double nuclear processes

From the processes discussed up till now, one can conclude the following: (a) it is advantageous if the wave vector (momentum) transferred through the intermediate state by Coulomb interaction has the maximum possible value, and (b) the appearance of resonance significantly increases the nuclear reaction rate. These conclusions led to a 4th-order, electron catalyzed double nuclear process, the graphs of which can be seen in Fig. 3. For a particular choice of the participants [66], resonances can be found in the processes of Fig. 3 (a) and (b). The resonance arises in line 4'. Moreover, the details of the calculation show that a large contribution to the counting rate is obtained if the energy of the electron in the final state is negligible compared with the energy of the total reaction. In other words, the main contribution to the counting rate is produced by final states in which particles 6 and 7 share the reaction energy.

It is supposed that particle 1 (1' and 1") is a quasi-free electron of the solid (a metal). Particle 2 is an ingoing free, heavy, positively charged particle of system B. Particles 3, 4, and 5 are heavy particles of positive charge that are localized in the solid. If processes of Fig. 3 (a) and (b) have resonance-like character [66], then the process of Fig. 3 (c) does not, and so its contribution to T_{fi} may be neglected. In that case, particle 4 is localized and its state is given by (31). Generally, in the electron catalyzed double nuclear reactions, two reactions are coupled, both of which may be capture reactions or reactions with two final fragments.

6.3. Nuclear power in Ni–H systems due to double proton capture

Extra heat production was observed in the Ni–H system by use of hot hydrogen gas [89,90]. The nuclear origin of the heat was proven with neutron detection [91]. It was shown in [66], that in gaseous Ni–H systems, the quasi-resonant electron catalyzed (double) proton capture of the Ni isotopes (the processes in Fig. 3) may have a high rate. The power generated by such nuclear processes, as calculated from our theory, is also considerable from a practical viewpoint. For the numerical details see [66]. The chemical-catalytic process producing atomic hydrogen [92] is not considered in [66]. It was supposed that the entire gas is atomic at the Ni surface. The obtained nuclear powers were consistent with observations [89,90].

6.4. Other results of third and fourth order reactions

In addition to the reactions just discussed, it is found that the coupled $d + d \rightarrow {}^4$ third order deuteron and fourth order electron catalyzed double nuclear processes have extremely large counting rates. The potential nuclear power has

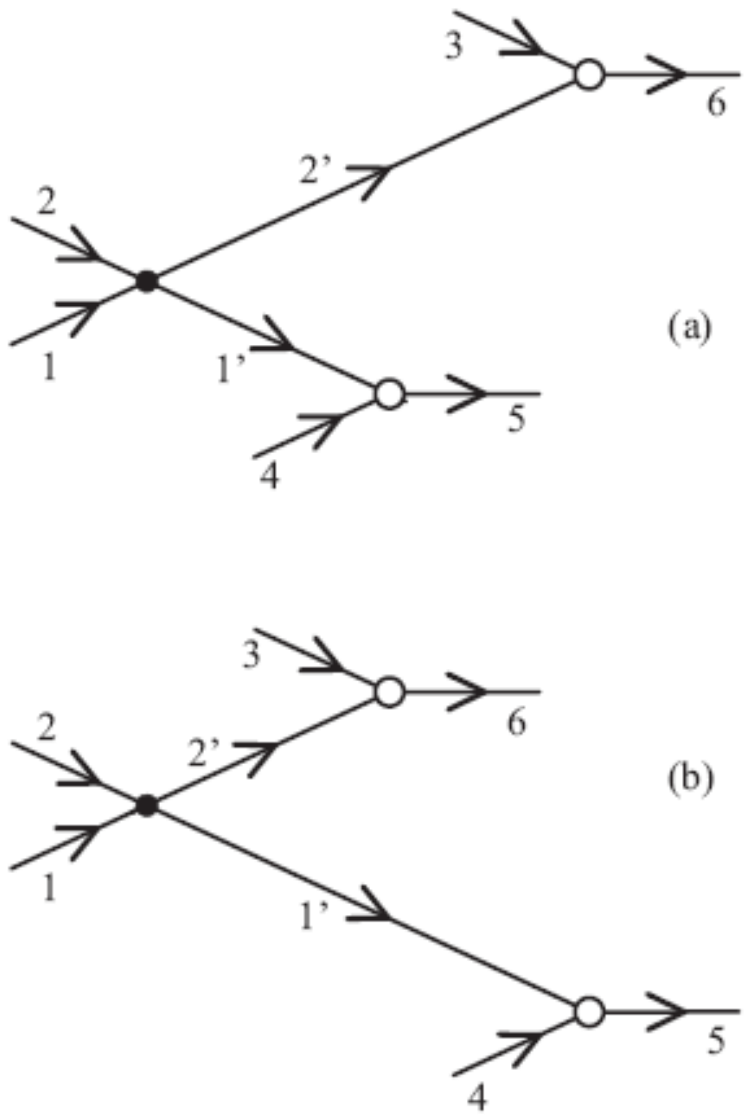

Figure 2. Graphs of quasi-resonant heavy charged particle Coulomb-catalyzed nuclear reactions. The filled dots denote Coulomb-interactions and the open circles denote nuclear (strong) interactions. The free particle 2 (e.g., p or d) belongs to system B. Localized particles 1, 3 and 4 belong to system A. All the particles are heavy and positively charged. From the point of view of the nuclear process, particles 1' and 2' are ingoing, particles 3 and 4 are targets, and particles 5 and 6 are reaction products. For the case discussed in [66], there is a resonance in process (a). Therefore its contribution to the rate is dominant, and the contribution of the process (b) is neglected.

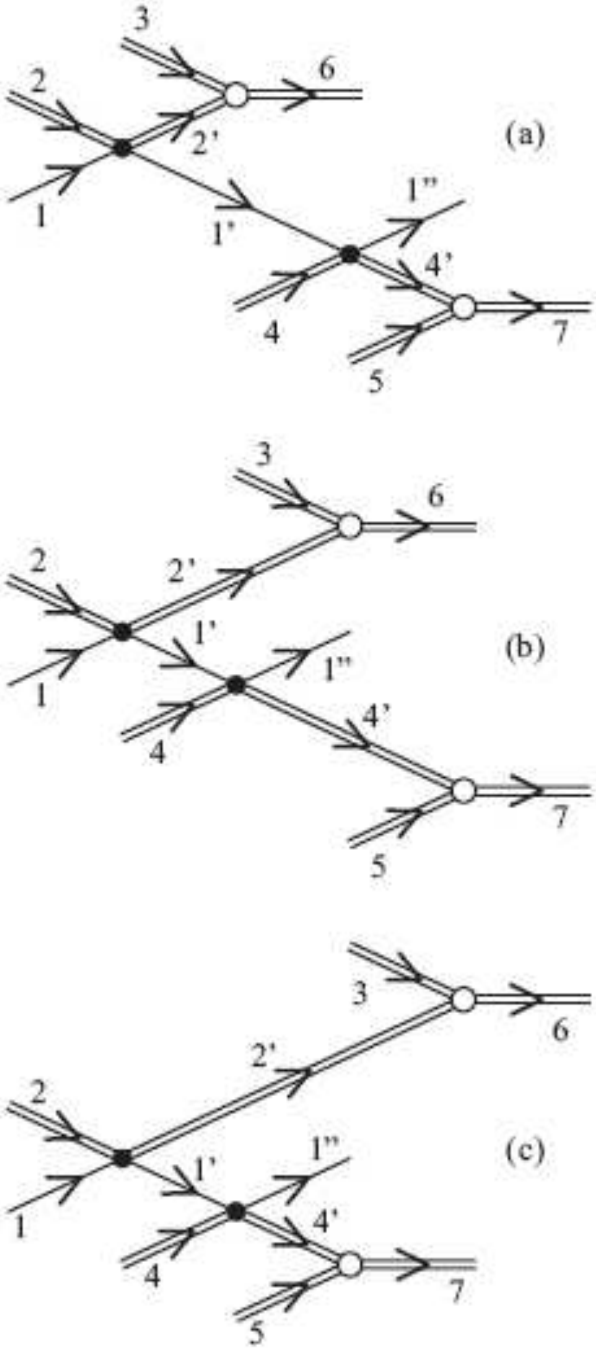

Figure 3. The graphs of quasi-resonant, electron catalyzed nuclear processes. The simple lines represent free (initial (1), intermediate (1') and final (1")) electrons. The doubled lines represent heavy, charged initial (free 2, bound 4) particles (such as p, d), their intermediate states (2', 4'), target nuclei (3, 5) and reaction products (6, 7). The filled dots denote Coulomb-interactions and the open circles denote nuclear (strong) interactions.

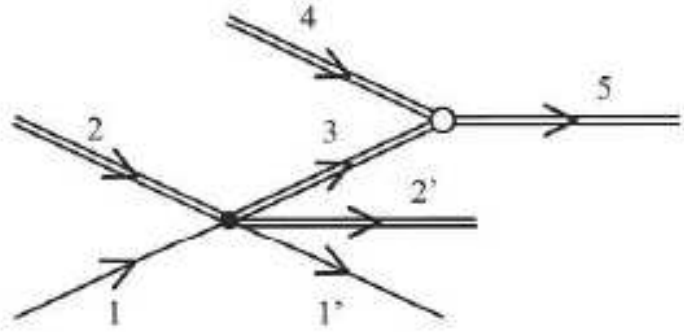

Figure 4. The graph of cooperative exchange processes (46). Particle 1 (q) and 1'(q') correspond to catalyzing charged particle, particle 2 is the nucleus which loses ${}^{A_3}_{z_3}w$ and becomes particle 2'. Particle 3 is the intermediate ${}^{A_3}_{z_3}w$. Particle 4 is the nucleus which absorbs ${}^{A_3}_{z_3}w$ and becomes particle 5. The filled dot denotes Coulomb-interaction and the open circle denotes nuclear (strong) interaction.

considerable magnitude from the point of view of practical applications [66]. The ${}^4_2$He production with $34.7\ \mathrm{MeV/He}$ obtained in 3rd order deuteron and 4th order electron catalyzed coupled $d+d \to {}^4_2$He and ${}^{A}_{46}$Pd$+d \to {}^{A+1}_{47}$Ag processes seem to fit well with the observed 32 ± 13 MeV/He value from LENR experiments [16]. However, it was pointed out in Section 5. that adequately large enough numbers of possible catalyzed nuclear reactions (e.g., p - and d-capture reactions in the case of all elements of the periodic table [84]) may happen and produce energy without emitting ${}^4_2$He. This possibility can explain the uncertainty in the emitted energy of ${}^4_2$He particles.

7. Cooperative Exchange Processes

Up to this point, the modification of the nuclear structure due to surroundings was not considered. However, Coulomb interactions and electromagnetic radiation may change the nuclear structure, e.g., they may break up (virtually) nuclei such as deuterons. Now these processes will be briefly considered. The treated processes have the following general form

$$q + {}^{A_1}_{Z_1}X + {}^{A_2}_{Z_2}Y \to q' + {}^{A_1-A_3}_{Z_1-z_3}\mathrm{V} + {}^{A_2+A_3}_{Z_2+z_3}\mathrm{W} + \Delta . \qquad (46)$$

Here q and q' denote any charged particle of the surroundings (e.g., bound and free electrons) and Δ is the energy of the reaction, i.e., the difference between the rest energies of the nuclei in initial $\left({}^{A_1}_{Z_1}X + {}^{A_2}_{Z_2}Y\right)$ and final $\left({}^{A_1-A_3}_{Z_1-z_3}\mathrm{V} + {}^{A_2+A_3}_{Z_2+z_3}\mathrm{W}\right)$ states. The intermediate particle (particle 3 in Fig. 4), which is exchanged, is ${}^{A_3}_{z_3}w$.

In process (46), the initial particle q (particle 1) Coulomb interacts with the nucleus ${}^{A_1}_{Z_1}X$ (particle 2). A recoiled particle q' (particle $1'$), the intermediate particle ${}^{A_3}_{z_3}w$ (particle 3) and the nucleus ${}^{A_1-A_3}_{Z_1-z_3}V$ (particle $2'$) are created due to this interaction. The intermediate particle ${}^{A_3}_{z_3}w$ (particle 3) is captured by the nucleus ${}^{A_2}_{Z_2}Y$ (particle 4) due to the strong interaction, forming the nucleus ${}^{A_2+A_3}_{Z_2+z_3}$W (particle 5). Hence, in process (46), the nucleus ${}^{A_1}_{Z_1}X$ (particle 2) loses the particle ${}^{A_3}_{z_3}w$, which is taken up by the nucleus ${}^{A_2}_{Z_2}Y$ (particle 4). The overall process is energetically allowed if $\Delta > 0$.

If particle ${}^{A_3}_{z_3}\mathrm{w}$ is a neutron, then the physical explanation of the virtual neutron stripping due to the Coulomb interaction is the following. The Coulomb interaction acts between the Z protons and particle q (e.g., an electron). The neutrons do not feel the Coulomb interaction. So one can say that the nucleus ${}^{A_1-1}_{Z}X$ is in fact stripped of the neutron due to the Coulomb interaction. In electric dipole coupling, the neutron has effective charge $q_n = -Z_1 e/A_1$ [93].

7.1. Cooperative internal conversion processes

If q in the initial state of (46) is a bound electron, then the reactions are called cooperative internal conversion processes (CICP). They were studied in [68], where the case of noble gases and, in particular Ne, was numerically investigated.

The cross section $\sigma_{bf}(A_1, A_2)$ of the bound-free (bf) electron transitions of CICP was determined with the aid of standard second order perturbation theory of quantum mechanics in the spherical shell model [94]. For the details, see [68]. In the numerical calculation, $V_0 = 50$ MeV was used [93] for the depth of a rectangular potential well which described the strong interaction. In the case of Ne, only the $e+\ {}^{21}_{10}\mathrm{Ne}+\ {}^{21}_{10}\mathrm{Ne} \rightarrow e'+\ {}^{20}_{10}\mathrm{Ne}+\ {}^{22}_{10}\mathrm{Ne} + \Delta$ reaction is allowed with $\Delta = 3.603$ MeV. The transition probability per unit time was estimated as $\lambda_1 > \lambda_1(K)$ taking into account the transition from the K shell of Ne. A cross section of $\sigma_{0bf,sh}(K) = 8.25 \times 10^{-45}\ cm^{-2}$ was obtained. Taking this for the half-life $\tau_{1/2,1}$ associated with the process, $\tau_{1/2,1} < 3.8 \times 10^{16}\ s$ ($1.2 \times 10^{9}\ y$) was obtained for a gas of normal state $\left(n = 2.652 \times 10^{19}\mathrm{cm}^{-3}, T = 273.15\,\mathrm{K}, p = 100\,\mathrm{kPa}\right)$. The estimated half-life is so long that the decay through CICP does not alter natural abundance of Ne to an observable degree. However, the rate is high enough to be measurable. ${}^{20}_{10}$Ne and ${}^{22}_{10}$Ne are mostly formed with energy near below $E_{10} = \frac{A_1+1}{A_1+A_2}\Delta_{\mathrm{Bi}} = 1.97$ MeV and $E_{10} = \frac{A_1-1}{A_1+A_2}\Delta_{\mathrm{Bi}} = 1.63$ MeV with wave vectors of opposite direction. Therefore, it is plausible to observe their creation by a coincidence measurement.

Cooperative internal conversion processes with proton and triton exchanges were also investigated [68]. There are other possibilities for realizing cooperative exchanges, when the exchanged heavy particle is d, ${}^{3}_{2}$He and ${}^{4}_{2}$He, but they were not investigated.

7.2. Results of electron catalyzed neutron exchange

In [67], two families of electron catalyzed reactions were investigated numerically:

$$e +\ {}^{A_1}_{28}\mathrm{Ni} +\ {}^{A_2}_{28}\mathrm{Ni} \rightarrow e' +\ {}^{A_1-1}_{28}\mathrm{Ni} +\ {}^{A_2+1}_{28}\mathrm{Ni} + \Delta \tag{47}$$

and

$$e +\ {}^{A_1}_{46}\mathrm{Pd} +\ {}^{A_2}_{46}\mathrm{Pd} \rightarrow e' +\ {}^{A_1-1}_{46}\mathrm{Pd} +\ {}^{A_2+1}_{46}\mathrm{Pd} + \Delta. \tag{48}$$

With neutrons in the uppermost energy level of ${}^{A}_{28}$Ni and ${}^{A}_{46}$Pd isotopes, we used the $1p$ shell model states in the cases of $A = 58 - 60$ and the $0f$ shell model states in the cases of $A = 61 - 64$ of the Ni isotopes and the $0g$ shell model states in the cases of $A = 102 - 104$ and the $1d$ shell model states in the cases of $A = 105 - 108$ of the Pd isotopes [94].

It was found that in the spherical shell model the processes

$$e +\ {}^{61}_{28}\mathrm{Ni} +\ {}^{58}_{28}\mathrm{Ni} \rightarrow e' +\ {}^{60}_{28}\mathrm{Ni} +\ {}^{59}_{28}\mathrm{Ni} + 1.179\,\mathrm{MeV} \tag{49}$$

and

$$e +\ {}^{108}_{46}\mathrm{Pd} +\ {}^{105}_{46}\mathrm{Pd} \rightarrow e' +\ {}^{107}_{46}\mathrm{Pd} +\ {}^{106}_{46}\mathrm{Pd} + 0.342\,\mathrm{MeV} \tag{50}$$

have the largest cross section $\sigma_{Sh} = 0.088/E_{ie}\ \mu b$ and $\sigma_{Sh} = 0.26/E_{ie}\ \mu b$, respectively, with E_{ie} the energy of the electron initially given in MeV. In this case, the ${}^{60}_{28}$Ni and the ${}^{59}_{28}$Ni isotopes take away 0.585 MeV and 0.594 MeV, and the ${}^{107}_{46}$Pd and the ${}^{106}_{46}$Pd isotopes take away 0.170 and 0.172 MeV, respectively.

Reactions (48), and especially (50), may be connected to the results of an unusual LENR experiment [95] in which the cathode was a wire of Pd 50 μm in diameter. It was configured to have a current flowing along its length of 250 cm, as well as between it and the anode. In that experiment, a large power density of 50 kW/cm^3 was observed but that experiment has not been repeated [13]. However, the origin of the obtained large power density in that and similar experiments is open to question. Perhaps it is due to electron catalyzed reactions caused by the electron current in the cathode, or it may be due to the increased quasi-free deuteron number density caused by electromigration [96].

7.3. Photo-induced nuclear cooperation: the cooperation factor

Finally, still considering cooperative processes, photo-induced nuclear cooperation is worth mentioning. In a recent report [97], observations of nuclear activity in deuterated materials subjected to a low-energy photon beam was reported. Importantly, the photon energy was less than the deuteron binding energy $B = 2.225$ MeV.

The results of [97] indicate that to induce nuclear activity the simultaneous presence of deuterons and a photon flux is necessary. In control experiments with samples made from H, nuclear activity did not appear [97]. So the observed phenomenon may be ascribed to 'virtual' photo-disintegration of deuteron, i.e., the process responsible for nuclear activity may be one in which electromagnetic radiation virtually breaks up deuterons, and then the virtually-free neutron is captured by another nucleus [98]. The overall reaction is

$$n_\gamma \gamma + \ d + \ {}^{A_2}_{z_2}X \rightarrow (n_\gamma \pm 1)\,\gamma + \ p + \ {}^{A_2+1}_{z_2}X + D_j, \tag{51}$$

which was called photo-induced nuclear cooperation with neutron exchange. (The term 'virtual' refers to the intermediate state in standard second order perturbation theory.) Here γ denotes photon, n_γ is the number of γ photons initially present, d is deuteron which is 'virtually' broken up due to electromagnetic interaction, ${}^{A_2}_{z_2}X$ stands for the cooperating (target) nucleus which absorbs the 'virtual' free neutron, ${}^{A_2+1}_{z_2}X$ denotes final nucleus (of $A_3 = A_2 + 1$) and D_j is the energy of the reaction.

A special case of (51) is when $n_\gamma = 0$, i.e., when initially photons are not present. In this case, (51) reads

$$d + {}^{A_2}_{z_2} X \rightarrow \gamma + p + {}^{A_2+1}_{z_2} X + D_j. \tag{52}$$

This reaction was called cooperative spontaneous γ emission with neutron exchange.

The transition probability per unit time and the cross section calculation for processes (51) and (52) were based on theoretical results obtained during cross section calculations of real photo-disintegration of the deuteron [29,99,100]. They were carried out with the aid of standard second order perturbation theory of quantum mechanics [74]. It was found [98] that the full rate of cooperative spontaneous γ emission is many orders of magnitude larger than the rate of photo-induced nuclear cooperation, which could produce a γ source. Investigating the observations [97], it was found that the observed activity cannot be achieved by irradiation of samples by a γ flux. Perhaps, cooperative spontaneous γ emission may be responsible for the observed nuclear activity.

In [98], an important quantity, the cooperation factor F_{coop}, was introduced. It takes into account contributions to the counting rate, which come from cooperating nuclei located at different distances. It was found that cooperation factor may considerably decrease rates and cross sections of cooperative processes between localized participants. So, in this case it must be taken into account.

8. Importance of Plasma-Like States

Plasmas have been mentioned a few times earlier in this review. However, we have yet to make clear either their relationship to LENR in general, or the role they play in our theoretical work. This section starts with a very brief summary of how plasmas have been involved in past LENR experiments. Then, we review why plasmas are a significant part of our theoretical work.

8.1. LENR experiments involving plasmas

Both conventional high temperature plasmas and plasmas in condensed matter have been part of many LENR experiments. Plasmas consisting of electrons and positive ions exist at a wide range of temperatures. The use of ultrasonically-induced cavitation bubbles to introduce protons and deuterons onto and into metal targets involved hot plasmas. Such experiments produced evidence of heat generation, which was attributed to LENR [101]. More common low temperature glow discharge plasmas have also caused interactions between hydrogen isotopes and metals. Such experiments produced strong evidence of tritium generation [102]. The experiments just noted involved low and high density media.

Most LENR experiments have involved condensed matter of some type, many in plasma-like states with mobile charges of both signs. Molten salts can be thought of as plasmas of mobile negative anions and positive cations. Early experiments with electrolytes of molten salts resulted in reports of significant LENR heat [103]. Ordinary liquid electrolytes, with salts dissolved in light or heavy water, share a significant characteristic with conventional plasmas because they consist of mobile negative and positive charges. Although shielded by hydration, they respond to fields between the electrodes. Such electrolytes have been used in hundreds of LENR experiments, which produced LENR heat and evidence of transmutations.

Solid-state plasmas have been involved in LENR experiments. Mobile conduction electrons in metals and alloys are inevitably part of the cathodes and other metallic components in LENR experiments. They have high densities. Similarly, electrons and holes in semiconductors share many characteristics with low density hot plasmas. Their density can vary widely from low to high values, depending on the doping. Semiconductors have been part of only a few LENR experiments. One involved a graded mixture of semiconductor and metallic particles, which give some evidence of voltage production [104]. Proton conductors are insulating compounds with relatively open structures, through which hydrogen isotopes can move due to fields. Some experiments with proton conductors have given evidence of LENR [105].

It is possible to consider protons and deuterons on and within metals and alloys as a type of plasma due to their high mobility. Such isotopes on the surface are subject to applied fields, as well as to diffusion. In the interior of metals, where fields are usually shielded, diffusion can still produce relatively rapid motion of hydrogen isotopes.

Ordinarily, the ions on or in a lattice are not thought of as analogous to the ions in gaseous plasmas, because they are localized in position in a lattice. However, we view the hydrogen isotopes within solids similar to the ions in gaseous plasmas, due to their high mobility. That mobility has a clear foundation. Hydrogen isotopes in metals do not have bound electrons, as do all other elements in the periodic table in a lattice. They are transiently screened by the free electrons of the conduction band, again much as in a gaseous plasma. The lack of bonding electrons on hydrogen isotopes in metals gives them sizes on the scale of femtometers, the normal nuclear size scale, since they are only nuclei. Their diameters are not on the scale of the size of other ions, that is about one-tenth of a nanometer. The small size is at the root of their very high diffusion coefficients [106] and the behavior of proton conductors [107. Protons and deuterons in materials that exhibit LENR are much like the positive ions in ordinary plasmas with a significant exception. Their motions are not random in all directions, but are constrained by the directions available in a lattice. However, they are still very mobile.

8.2. Roles of plasmas in the theoretical work

The mobility of nuclei is fundamental to the occurrence of the key mechanisms discussed in earlier sections of this paper. Since we desire two important conditions, (a) the mobility, which is often called a quasi-free state, and also (b) high densities to achieve high reaction rates, we have primarily considered plasmas in low temperature condensed matter.

The mechanisms we have developed and elaborated do not have to involve high speed, that is, energetic or hot, nuclei. Importantly, they are active in and explain low temperature nuclear reactions. However, some nuclear mobility is still required, such as exists in plasmas. Our key mechanism, the three-body catalytic reaction, requires reactants of quasi-free state. There is no requirement for the initial motion of the catalyzing nucleus, however, its quasi-free motion is allowed. The high mobility of protons and deuterons on and in metals and alloys is critical to production of LENR and to our explanation of LENR. Our view of the collection of hydrogen isotopes on or within lattices as a plasma of mobile nuclei is not common, but is fundamental to our developments and results.

However, some of our calculations have shown that the impurities, if they are present in conventional hot plasmas of fusion power experiments, might also catalyze nuclear reactions. We dealt with the case of such a dense and hot plasma, which is very similar to the plasmas created in inertial confinement fusion experiments [108,109]. Our theoretical results [71,21] indicate that the presence of impurities of high charge number and of large number density, which are strongly prohibited now since they induce high radiation losses, may be advantageous. It is because the mechanism we considered might drastically reduce the temperature needed to induce and maintain nuclear (mainly fusion) reactions in such plasmas. This possibility is not on a par with our fundamental explanation of the root causes of LENR. It is introduced because of the potential positive role of impurities within high temperature fusion plasmas, and more importantly, the positive effect of possible interactions of ions from hot plasmas with the walls of containment systems, if they are possible.

9. Comparisons with LENR and dd Fusion Data

The earlier parts of this paper sought to explain the concepts, and results based on them, as obtained from the research program of two of us. Empirical data on LENR and on the enhanced deuteron fusion cross sections at low beam energies were introduced occasionally, as appropriate. The main features of LENR, which seem to be explained and are mentioned above, are the followings:

(a) Nuclear reactions may occur at low energy.
(b) Nuclear transmutations may occur across periodic table in LENR experiments.
(c) Heat production without considerable emission of γ radiation is possible.
(d) Excess heat goes hand in hand with helium production in LENR experiments.
(e) A current density threshold may appear in electrolytic-LENR experiments.
(f) Energy production in Ni–H experiments may be explained.
(g) Connection of accidental processes (bursts, explosions and craters) with Boson Induced Fusion and parametric-like loss mechanism may be made.

Now, we deal with some of LENR data in more detail, but we invert the approach to focus on the experimental side, i.e., on the many characteristics of laboratory data on LENR, and also on the low energy deuteron fusion cross sections. The theoretical works are reintroduced where they fit. It is hoped that this section will enable readers to see that we have made substantial and successful contact between the results of our theoretical work and the large amount of empirical information from laboratory research on LENR. We begin by focusing on LENR. Then, we turn to the enhanced cross sections, which were also considered theoretically with some success.

9.1. Low Energy Nuclear Reactions

The voluminous empirical experience for and about LENR can be sorted into different categories of varying strength. The widely and well established ability to cause nuclear reactions on or in solids by using chemical energies, without emission of intense energetic gamma and neutron radiations, is in the top category. Those two observations were referred to as “miracles” by the earlies critics of cold fusion. The subsequent three decades of LENR experiments have shown both the absence of radioactive products after LENR, and the high variability of LENR measurements. Those two observations are strongly supported by thousands of experiments, hundreds of which have given evidence for LENR. They involve different solids, notably palladium and nickel, and both protons and deuterons. In the second category are observations that have been reproduced at multiple laboratories, notably heat generation and transmutations, including some parametric variations. The last category includes observations that have yet to be reproduced properly, but are still worth attention, sometimes because of the reputation of the scientists involved. We discuss each of the groups in turn.

The occurrence of LENR in experiments with solid components, without emission of significant intensities of neutrons or gamma rays, is well established [14]. The observations cannot be explained by chemistry. The three-body mechanism we conceived and explored offers explanations for both the production of LENR in low energy circumstances and the absence of γ radiation [21,65]. This mechanism requires adequately high densities of all three of the involved nuclei, the two reactants and the catalyzing particle. This explains the need for solid components, such as electrodes in electrolytic LENR experiments, which usually provides the largest number density of the three involved nuclei. The theoretical work reviewed above shows that it is possible for LENR to occur in both palladium and nickel [69,70] (and other metals), and that both protons and deuterons can enter into LENR [21,84].

The absence of radioactive products after LENR experiments, is not absolute, because tritium is produced in some experiments, probably by catalyzed $d(d,t)p$ reactions. However, the amount of the radioactivity in LENR products is vastly smaller than in the products of fission reactions, and that expected in fusion reactors due to activation of materials near the hot plasmas. In a recent paper [84], we computed nickel-catalyzed LENR rates for the formation of product nuclei in both their ground and first excited states. The probability of formation of a nucleus in the excited states was found to be substantially less than the formation in the ground state. This occurs because the reaction energy decreases with the excitation energy, and therefore, the possibility of recoil decreases. The calculations did not take into account angular momentum conservation, which may account for further decrease in the production of excited states. This is a topic that needs much further exploration.

The three-body mechanism also provides one of the rationales for the inconsistency of LENR experiments. If the necessarily high triple number density product is not achieved on or in some parts of the involved solids, LENR will not be seen. The establishment and maintenance of the right local conditions, what Storms calls the Nuclear Active Environment, is necessary, but not easy. It depends on experimental details, including the composition and structure of the materials, and also on the protocols used.

Diversity of the results of seemingly similar electrolysis experiment may have a further reason. Important quantities like, e.g., the pH value and its distribution in the case of electrolysis, and also detailed chemical composition of all parts of the experimental arrangement, are generally not measured or reported. However, they influence or determine the local rate of LENR. The wide variety of possible reactions means that the outcomes of experiments can vary widely, when LENR are produced [21, 84].

The second category of LENR evidence includes the correlation of heat and helium production in many experiments. Some of the best work indicates that approximately 32 MeV of energy are released for each helium nucleus produced [110]. The theoretical work reviewed in earlier sections shows that there are several exothermic nuclear reactions that produce helium [21, 84]. Some of the reactions would produce 34.7 MeV/He [66]. Moreover, (p,α) and (d,α) reactions are energetically allowed with many isotopes of the periodic table. Altogether, the proportionality of excess heat with ^{4}He production is clarified. Hence, it is not necessary to focus on dd fusion reactions to understand helium production and its relation to heat generation.

There are other observations of the correlation of excess heat with two of the parameters in LENR experiments, which date from the earliest days of the field and which have been reproduced in other experiments. The first is a requirement for high loading of deuterons into palladium. It was reported by two laboratories in 1992 that the production of LENR heat scales quadratically with the fraction of octahedral sites in palladium that are occupied by deuterons, above a threshold of about $u = 0.85$ with u the deuteron over metal ion number density [111]. This feature may be easily explained by the rate and power density equations of the three-body mechanism. Since deuterons are targets and reactants as well, their number density enters twice (quadratically) in the triple product [21,71]. The second well-established empirical requirement was also found in electrochemical experiments. LENR production requires an electrolysis current density at the cathode surface of at least 100 mA/cm^2 [1,111,112]. This observation was obtained in d filled Pd. The threshold in the current density of electrolysis may be explained by the threshold condition of the BIF mechanism [47].

Other systematic laboratory LENR experiments involved variation of the temperature of electrochemical cells and gas reaction chambers. It was found in six experiments with palladium or nickel, and protons or deuterons in various combinations that the generation of LENR energy depended exponentially on the inverse of the temperature [115].

This so-called Arrhenius behavior of the generation of excess power P_{exc} is certainly due to nuclear reactions. The observed $\ln P_{\text{exc}} \sim 1/T$ temperature dependence in the case of electrolysis of deuterized materials [113,114], where T is the absolute temperature, may partly be attributed to the number N_3 of quasi-free deuterons, which is temperature dependent [70]

$$N_3\left(T\right) = N_1 u \mathrm{e}^{-\frac{E}{kT}} \mathrm{e}^{-\frac{\varepsilon}{kT}}, \tag{53}$$

where the number of filled lattice points of the d sub-lattice is $N_1 u$ with N_1 the number of possible host-lattice sites, E is the activation energy of the deuteron necessary for it to be quasi-free in the host lattice, and ε is its quasi-kinetic energy. So, $N_3(T)$ gives the number of deuterons, which are within the lattice but are delocalized, so that they can move quasi-freely within the lattice, and take part in the processes discussed. The movement of deuterons in a lattice is a problem of diffusion, as it was pointed out recently [114].

The top evidence for LENR is the occurrence of nuclear transmutations, which cannot happen without nuclear reactions. Many LENR experiments have shown the production of elements, which were not present at the start of the experiments [116]. Changes in isotope ratios have also been measured [117]. Our theoretical work already reviewed offers an explanation for such transmutations. A mechanism for participation of elements across the periodic table in LENR was offered [84]. Changes in isotope ratios in specific experiments were also rationalized [69]. Some LENR research has involved the measurement of the abundance of elements across the periodic table before and after experiments. Two very different experiments showed that the production rate of the created new elements varies with atomic mass in the same fashion [23, 118]. We note that a recent paper, which described diverse experimental efforts to produce LENR, neglected the topic of nuclear transmutation [119].

The third category of LENR evidence lacks reproduction in multiple laboratories. However, there is no reason to dismiss all such reports. We cite a few of them to illustrate work that needs more experimentation and further theoretical consideration.

In one LENR experiment, the cathode was examined with an infrared video camera, which permitted recording of the spatial locations of the appearance and disappearance of hot spots [120]. Although the measurements were near the limit of sensitivity of the instrument, they showed twinkling on and off of small hot regions distributed over much of the cathode surface. Hence, the temperatures obtained from the infrared data indicated very high power densities, which could only be explained by nuclear energy releases [58]. The same group that did the infrared imaging experiment, also deposited Pd -d on a microphone. They recorded bursts of sound, again indicative of rapid energy releases [121].

Hot spots and accidental processes (bursts, explosions and craters) have been reported in many LENR experiments [122, 123]. They may be connected not only to BIF reactions, but to a published speculation on the possibility of LENR chain reactions [124]. As was shown in [21] and [84], a very huge number of catalyzed nuclear reactions can occur as a consequence of the three-body mechanism and its associated recoil. The products of such reactions have kinetic energy in the MeV range. These energetic products can take place in further regular nuclear reactions, establishing the possibility of nuclear chain reactions. Moreover, the successive operations within the BIF and parametric amplification mechanisms are unlike a conventional fission chain reaction, but they share a common feature of amplification.

The results just noted focus attention to BIF processes again. In view of the above perhaps BIF may have more general role in excess heat production. It was clarified that a great number of nuclear reactions can take place in catalytic manner. Calculations also indicate that the coupling due to catalyzed processes in the laser-like mechanism (the recalculated $V_{ab,jl}$ and $V^*_{ab,jl}$ in (16)) are expected to be much stronger than the coupling used in [47]. The much stronger coupling may drastically reduce the threshold conditions for BIF. Consequently, they may take place more frequently, and with moderated amplitude too. The amplitude of the BIF process is proportional to generated heat. Thus, BIF may have importance not only in burst like processes. Returning to the infrared and acoustic experiments, where the cathode was composed of very small crystallites of Pd -d produced in place by co-deposition, many different possible orientations of crystal planes were created. These would offer many possibilities for building up natural resonators for BIF. The occasional appearance of heat production, if it is connected to BIF, may be understood as due to fluctuations of pumping, which is the current density at the surface of the cathode. In experiments in which BIF plays central role the depressed production rate of γ, t , n and ^{3}He may be expected.

Rapid energy release in bursts has been noted already in calorimetric experiments, and in the formation of craters in materials, which are evident after LENR experiments. They have also happened in some noteworthy experiments. Pulses of heat measured in one calorimeter experiment occurred at seemingly random times, with highly variable amplitudes [125]. However, the authors found that a plot of the number of pulses with specific excess powers (less than 0.5 W) had a $1/f$ character, where f is the frequency of their occurrence. Such a behavior may be expected if the pulses are due to BIF. In this case, if a pulse of large excess power is produced, then a large number of the localized deuterons, which take place in the formation of the pulse, is utilized. Then, the system needs longer waiting time to be filled up compared to the case of a pulse of smaller excess power. The system needs time after each pulse to build up the population inversion (the necessary number density of localized deuterons), which is needed for the next pulse. The other crucial quantity is the pumping intensity, which is the current density of the electrolysis, the flux of the ingoing deuterons. It may happen that, if the local current density becomes an appropriately large value due to fluctuation, then BIF may start at a lower localized deuteron number density, producing lower excess power.

9.2. Enhanced low-energy dd fusion cross sections

In addition to the two core and related problems raised by LENR experiments, there was the unsolved riddle of the well-established enhancement of dd fusion cross sections at low (keV) beam energies [28]. Figure 2 of [82] gives examples of such data for a few different target materials. Such enhancements, which sometimes approach a factor of 100, have been part of the literature on LENR for many years [126-132]. However, the relationship between the larger cross sections and LENR has never been clarified. We found [21, 83, 69] that the mechanisms, which were studied for the understanding of LENR, are also able to explain the fusion cross section enhancements, the cause of which was unclear. This strengthens the case for the viability of our mechanisms, as well as enabling a basic understanding of the enhanced cross sections.

10. Summary

We have reviewed 17 years of theoretical research aimed at understanding 31 years of empirical data on LENR. Along the way, several mechanisms were explored, among which the most important is a three-body mechanism. It gives the clearest explanation of the two main features of LENR. The first is how LENR can occur at all, that is, how it is possible to cause nuclear reactions by use of chemical energies. The second is the absence of energetic radiation during LENR. The three-body mechanism can be viewed as a form of nuclear catalysis, where one nucleus of the surroundings enables LENR, and it and the nuclear product(s) carry off the nuclear reaction energy to heat the lattice by numerous inelastic collisions. Diverse nuclei can play the catalytic role. The work has shown how both protons and deuterons can participate in LENR, not only with light nuclei, but with elements across the periodic table. This explains some of the voluminous LENR data on transmutations. In this section, we summarize some of the highlights, starting with the reason why LENR is thought to be possible.

The very small cross sections, essentially the forbiddenness of nuclear reactions of heavy particles with like charges, originates from the $\lim_{\varepsilon\to0}\sigma(\varepsilon)=0$ variation of the cross sections. It determines the disappearing rate of nuclear reactions in the $\varepsilon\to0$ limit. However, by the analogy with forbidden optical transitions of atomic physics, the forbiddenness of nuclear reactions led to a general statement. It asserts that any perturbation may resolve the forbiddenness, and the cross section modified by a perturbation must be calculated at least up to second order according to the rules of quantum mechanics [21]. This statement is valid for all nuclear reactions having vanishing cross sections in the $\varepsilon\to0$ limit. Importantly, it applies to low-energy nuclear reactions of charged particles, in general.

The strongest perturbation, which must be taken into account, is the Coulomb potential, which is created by any charged particle (mainly a nucleus) of the surroundings. As a consequence, a huge number of forbidden nuclear reactions (see (22) and (23) with F Fig. 1 and (46) with Fig. 4) and also their coupling (see Figs. 2 and 3) may have considerable cross section because of Coulomb-catalysis of a charged particle within the surroundings. In all of the above reactions, heavy charged particles of nuclear energy (MeV order of magnitude) are created, which are potentially able to take part in subsequent ordinary nuclear reactions. The wide variety of possible nuclear reactions means that the emphasis on dd fusion reactions in the literature on LENR is no longer needed or desirable. We have shown that what was, and sometimes still is called "cold fusion" is a sub-case of the broader field of low energy nuclear reactions.

Moreover, as a consequence of Coulomb perturbation, nuclear reaction cross sections are proportional to n_1 and z_1^2, as in (35). Hence, increases of the density of the Coulomb catalyzing material and its charge number z_1 are advantageous, if one wants to reach the possible maximum nuclear reaction cross sections and power densities for LENR. This result explains the efficacy of using condensed matter, that is, why low energy nuclear reactions in solids and liquids, such as in aqueous solutions during electrolysis, are qualitatively different than nuclear reactions at high energies in any media. It makes clear why high average or local loadings of deuterons into Pd are so favorable to LENR, when both the deuteron and catalyzing metal number densities have large values. However, it can be emphasized that dense plasma states may also be advantageous, if one desires to achieve high power densities.

We have shown that p - and d-capture reactions (22) are possible with all the elements of the periodic table [84] , which explains the observations of diverse nuclear transmutation products after LENR experiments.

The proposed laser-like BIF process of nuclear fusion in deuterized Pd [47], the loss mechanism similar to a parametric oscillator, and the possibility of favorable deuteron concentrations [48] were all obtained as a consequence of the quantized modes selected by a crystal resonator. Collectively, they call the attention to the importance of the boson character of the initial and final participants of nuclear fusion reaction in deuterized Pd, and the potential value of adaptation of methods from quantum electronics. BIF processes and the new loss mechanism may be formed accidentally, e.g., due to the fluctuation of the current density during electrolysis, resulting in uncontrollable and accidental appearance of bursts of LENR.

We have achieved substantial understanding of the primary characteristics of LENR by consideration of the three-body and other nuclear mechanisms. It is thought that these mechanisms mostly contribute to resolution of the main puzzles of LENR observations, the basis of which is part of nuclear physics. What happens in LENR experiments includes the joint actions of diverse kinds of chemical and solid-state processes, as well as nuclear mechanisms. It is clear that LENR are very complex, so what is measured during and after LENR experiments depends on details of the experiments, many of which are not known. For example, nuclear transmutations and changes in isotope abundances may depend on the spatial distributions of constituent impurities within experimental materials. And, the distribution of materials and variations in conditions, which influence LENR, are time dependent. So, there remain numerous problems connected to electrochemistry, hot gases, plasmas, solid state and surface physics, and materials science, which need clarification. There is still much research to be done to quantitatively understand what happens in concrete LENR experiments.

Turning from LENR to astrophysics, we note that the phenomenon, which we developed and examined to understand LENR, and discussed above, may have significant astrophysical impacts [133]. The evolution of the abundance of particular nuclei in both cosmological and stellar processes is determined by a system of coupled, nonlinear ordinary differential equations (called the network) [134]. Thorough determination and development of the network of equations requires taking into account every process that produces or destroys nuclei with considerable counting rate density (called the rate in [134]). However, reactions with non-zero counting rate densities have been omitted from earlier nuclear reaction network calculations. Such reactions include Coulomb catalyzed forbidden reactions ((22), (23), and in the case of catalysis by an electron, ${}^{A_1}_{z_1}V$ and ${}^{A_1}_{z_1}V'$ is changed to e and e' in them), which have high counting rate densities. The counting rate densities for such reactions, which are proportional to the product of the number densities $n_3n_2n_1$ of the initial particles (see (36)), can have considerable magnitude if the product $n_3n_2n_1$ reaches appropriately high values, as in the early stages of the universe and in stellar environments. Therefore, the Coulomb catalyzed versions of forbidden nuclear reactions must not be omitted from astrophysical calculations, since they can drastically change some of the time scales in astrophysics.

The number of reactions in question, and the number of processes which can be modified by them, are both enormous. Catalyzed capture reactions, and catalyzed reactions with two and three final fragments, can have cross section of considerable magnitude. Beside the catalyzed $p(p, e^{+}\nu)d$, ${}^{3}He({}^{3}\mathrm{He}, 2p)\alpha$ and $p + d \to {}^{3}$He reactions, which are important for cosmological models, almost all the basic reactions in every burning chain important to stellar evolution have catalyzed versions. Therefore, it is thought that the ideas reviewed in this paper might have two effects: (a) they require reconsideration of quantitative evaluations of cosmological and stellar networks of equations, and (b) they may help with finding solutions to problems remaining in determination of the age of some stars, for example, the recent observations of HD 140283 [135].

References

[1] M. Fleischmann, S. Pons, Electrochemically induced nuclear fusion of deuterium. *J. Electroanal. Chem.* **261**(1989) 301-308. https://doi.org/10.1016/0022-0728(89)80006-3

[2] S.E. Jones, E.P. Palmer, J.B. Czirr, *et al.*, Observation of cold nuclear fusion in condensed matter. *Nature (London)* **338** (1989) 737-740. https://doi.org/10.1038/338737a0

[3] E. Kashy, W. Bauer, Y. Chen, *et al.*, Search for neutron emission from deuterium-loaded palladium. *Phys. Rev. C* **40** (1989) R1(R). https://doi.org/10.1103/PhysRevC.40.R1

[4] C.J. Benesh, J.P. Vary, Fusion rates of squeezed and screened hydrogenic nuclei. *Phys. Rev. C* **40** (1989) R495(R). https://doi.org/10.1103/PhysRevC.40.R495

[5] Z. Sun, D. Tománek, Cold fusion: How close can deuterium atoms come inside palladium? *Phys. Rev. Lett.* **63** (1989) 59. https://doi.org/10.1103/PhysRevLett.63.59

[6] K. Szalewicz, J.D. Morgan, III., H.J. Monkhorst, Fusion rates for hydrogen isotopic molecules of relevance for "cold fusion". *Phys. Rev. A* **40** (1989) 2824(R)-2827. https://doi.org/10.1103/PhysRevA.40.2824

[7] A.J. Leggett, G. Baym, Exact upper bound on barrier penetration probabilities in many-body systems: Application to "cold fusion". *Phys. Rev. Lett.* **63** (1989) 191. https://doi.org/10.1103/PhysRevLett.63.191

[8] C.T. White, D.W. Brenner, R.C. Mowrey, J.W. Mintmire, P.P. Schmidt, B.I. Dunlap, D-D (H-H) Interactions within the Interstices of Pd. *Jpn. J. Appl. Phys.* **30** (1991) 182. http://iopscience.iop.org/1347-4065/30/1R/182

[9] R.H. Parmenter, W.E. Lamb, Jr., More cold fusion in metals: corrected calculations and other considerations. *Proc. Natl. Acad. Sci. USA.* **87**(8) (1990) 3177–3179. https://doi.org/10.1073/pnas.87.8.3177

[10] J. Schwinger, Cold fusion: a hypotesis, *Z. Naturforsch.* **45A** (1990) 756. https://doi.org/10.1515/zna-1990-0528

[11] J. Schwinger, Nuclear energy in an atomic lattice.1. *Z. Phys. D - Atoms, Molecules and Clusters* **15** (1990) 221-225. https://doi.org/10.1007/BF01437184

[12] J.R. Huizenga, *Cold Fusion: The Scientific Fiasco of the Century* (Oxford University Press, USA, 1994).

[13] D.J. Nagel, The status of cold fusion. *Radiat. Phys. Chem.* **51** (1998) 653-668. https://doi.org/10.1016/S0969-806X(97)00230-2

[14] E. Storms, *The Science of Low Energy Nuclear Reaction, A Comprehensive Compilation of Evidence and Explanations about Cold Fusion* (World Scientific, Singapore, 2007). https://doi.org/10.1142/6425

[15] S.B. Krivit, J. Marwan, A new look at low-energy nuclear reaction research. *J. Environ. Monit.* **11** (2009) 1731-46. https://doi.org/10.1039/b915458m

[16] E. Storms, Status of cold fusion. *Naturwissenschaften* **97** (2010) 861-881. https://doi.org/ 10.1007/s00114-010-0711-x

[17] D.J. Nagel, Questions About Lattice Enabled Nuclear Reactions: Mechanisms and Materials. *Infinite Energy Magazine* **20** (118) (2014) 15-28.

[18] E. Storms, Introduction to the main experimental findings of the LENR field. Current Science **108** (4)**,** 535-539 (2015). DOI:10.18520/cs/v108/i4/535-539

[19] V.A. Chechin, V.A. Tsarev, M. Rabinowitz, *et al.*, Critical review of theoretical models for anomalous effects in deuterated metals. *Int. J. Theor. Phys.* **33**(3) (1994) 617–670. https://doi.org/10.1007/BF00670521

[20] D.J. Nagel, Expectations of LENR Theories. *J. Condensed Matter Nucl. Sci.* **26** (2018) 15–31.

[21] P. Kálmán, T. Keszthelyi, Forbidden nuclear reactions. *Phys. Rev. C* **99** (2019) 054620. https://doi.org/10.1103/PhysRevC.99.054620

[22] P. Kálmán, T. Keszthelyi, Anomalous internal pair creation, *Eur. Phys. J. A* **56** (2020) 205. https://doi.org/10.1140/epja/s10050-020-00202-z

[23] T. Mizuno, T. Ohmori, M. Enyo, Isotopic changes of the reaction products induced by cathodic electrolysis in Pd. *J. New Energy* **1**(3) (1996) 31.

[24] M.C.H. McKubre, S. Crouch-Baker, R.C. Rocha-Filho, *et al.*, Isothermal flow calorimetric investigations of the D/Pd and H/Pd systems. *J. Electroanal. Chem.* **368** (1994) 55-66. https://doi.org/10.1016/0022-0728(93)03070-6

[25] K. Alder, A. Bohr, T. Huus, *et al.*, Study of nuclear structure by electromagnetic excitation with accelerated ions. *Rev. Mod. Phys.* **28** (1956) 432-542. https://doi.org/10.1103/RevModPhys.28.432

[26] P. Marmier, E. Sheldon, *Physics of Nuclei and Particles*, Vol. 1 (Academic, New York, 1969), pp. 315-317.

[27] H.J. Assenbaum, K. Langanke, C. Rolfs, Effects of Electron Screening on Low-energy Fusion Cross Sections. *Z. Physik. A - Atomic Nuclei* **327** (1987) 461-468. https://doi.org/10.1007/BF01289572

[28] A. Huke, K. Czerski, P. Heide, *et al.*, Enhancement of deuteron-fusion reactions in metals and experimental implications. *Phys. Rev. C* **78** (2008) 015803. https://doi.org/10.1103/PhysRevC.78.015803

[29] J.M. Blatt, V. F. Weisskopf, *Theoretical Nuclear Physics* (Wiley, New York, 1952).

[30] J.H. Hamilton, *Internal Conversion Processes* (Academic, New York, 1966).

[31] J. D. Jackson, Catalysis of Nuclear Reactions between Hydrogen Isotopes by μ^- Mesons. *Phys. Rev.* **106** (1957) 330-339. https://doi.org/10.1103/PhysRev.106.330

[32] P. Kálmán, T. Keszthelyi, Solid state internal conversion. *Phys. Rev. C* **69** (2004) 031606(R). https://doi.org/10.1103/PhysRevC.69.031606

[33] P. Kálmán, T. Keszthelyi, Lattice effect in solid state internal conversion. *Phys. Rev. C* **79** (2009) 031602(R). https://doi.org/10.1103/PhysRevC.79.031602

[34] J.M. Ziman, *Principles of the Theory of Solids* (Cambridge University Press, Cambridge, 1964), pp. 148-150.

[35] M. Lipoglavšek, S. Markelj, M. Mihovilovič, T. Petrovič, S. Štajner, M. Vencelj, J. Vesić, Observation of electron emission in the nuclear reaction between protons and deuterons, *Phys. Lett. B* **773** (2017) 553–556. http://dx.doi.org/10.1016/j.physletb.2017.09.004

[36] P. Kálmán, T. Keszthelyi, Attractive d-d interaction via phonon exchange in deuterated Pd. *Nucl. Instr. and Meth. in Phys. Res. B* **240**(4) (2005) 781-789. https://doi.org/10.1016/j.nimb.2005.06.207

[37] P.L. Hagelstein, Theory for Anomalies in Metal Deuterides, *Trans. Am. Nucl. Soc.* **83** (2000) 359.

[38] P.L. Hagelstein, Models for anomalies in condensed matter deuterides. in *Condensed Matter Nuclear Science,* ed. by A. Takahashi, K-I. Ota, Y. Iwamura. Proceedings of the 12th International Conference on Cold Fusion, Yokohama, Japan, 27 November – 2 December 2005 (World Scientific, Singapore, 2006), pp. 441-453. https://doi.org/10.1142/6190

[39] P.L. Hagelstein, I.U. Chaudhary, Phonon models for anomalies in condensed matter nuclear science. *Current Science* **108**(4) (2015) 507-513. https://www.jstor.org/stable/24216595

[40] P. Kálmán, T. Keszthelyi, D. Kis, *Solid state modified nuclear processes*. *Eur. Phys. J. Appl. Phys.* **44** (2008) 297-302. https://doi.org/10.1051/epjap:2008167

[41] C. Kittel, *Quantum Theory of Solids* (Wiley, New York, 1963), pp. 148-149.

[42] O. Yoshinari, Origin of "Inverse Isotope Effect" of Hydrogen Diffusion in Palladium, *Defect and Diffusion Forum* **312-315** (2011) 295-300.
doi:10.4028/www.scientific.net/DDF.312-315.295

[43] G. Borrmann, Die Absorption von Röntgenstrahlen im Fall der Interferenz. *Z. Physik* **127** (1950) 297-323. https://doi.org/10.1007/BF01329828

[44] B.W. Batterman, H. Cole, Dynamical Diffraction of X Rays by Perfect Crystals. *Rev. Mod. Phys.* **36** (1964) 681. https://doi.org/10.1103/RevModPhys.36.681

[45] A. Schüller, S. Wethekam, H. Winter, Diffraction of Fast Atomic Projectiles during Grazing Scattering from a LiF(001) Surface. *Phys. Rev. Lett.* **98** (2007) 016103. https://doi.org/10.1103/PhysRevLett.98.016103

[46] F. Aigner, N. Simonović, B. Solleder, *et al.*, Suppression of Decoherence in Fast-Atom Diffraction at Surfaces. *Phys. Rev. Lett.* **101** (2008) 253201. https://doi.org/10.1103/PhysRevLett.101.253201

[47] P. Kálmán, T. Keszthelyi, D. Kis, Boson induced nuclear fusion in crystalline solids, *Eur. Phys. J. Appl. Phys.* **50** (2010) 31101. https://doi.org/10.1051/epjap/2010053

[48] P. Kálmán, T. Keszthelyi, Loss-mechanism and favorable deuteron concentrations of boson induced nuclear fusion. *Int. J. Nucl. Energy Sci. Techn.* **6** (2011) 213-223. https://doi.org/10.1504/IJNEST.2011.043396

[49] M. Davidson, Theories of Variable Mass Particles and Low Energy Nuclear Phenomena, *Found. Phys.***44** (2014) 144-174.
https:// doi.org/10.1007/s10701-014-9774-4

[50] M. Davidson, Variable mass theories in relativistic quantum mechanics as an explanation for anomalous low energy nuclear phenomena, *Journal of Physics: Conference Series* **615** (2015) 012016.
https:// doi.org/10.1088/1742-6596/615/1/012016

[51] M. Davidson, Off-mass-shell Particles and LENR, *J. Condensed Matter Nucl. Sci.* **19** (2016) 46–55.

[52] H.M. Nussenzveig, *Introduction to Quantum Optics* (Gordon and Beach, London, 1973).

[53] C. Cohen-Tannoudji, B. Diu, F. Laloë, *Quantum Mechanics*, Vol. 1. (Wiley, New York/English version/, Hermann, Paris, 1977).

[54] P.W. Milonni, J.H. Eberly, *Lasers* (John Wiley, New York, 1988).

[55] M.J. Gillan, Quantum transition state theory and the diffusion of hydrogen in metals. *Journal of the Less Common Metals* **172–174** B (1991) 529-537.
https://doi.org/10.1016/0022-5088(91)90173-2

[56] P.A. Mosier-Boss, S. Szpak, The Pd/ ^{n} H system: Transport processes and development of thermal instabilities. *Il Nuovo Cimento A* **112**(6) (1999) 577–585. https://doi.org/10.1007/BF03035869

[57] S. Szpak, P.A. Mosier-Boss, C. Young, *et al.*, Evidence of nuclear reactions in the Pd lattice. *Naturwissenschaften* **92** (2005) 394–397. https://doi.org/10.1007/s00114-005-0008-7

[58] D.J. Nagel, Characteristics and Energetics of Craters in LENR Experimental Materials. *J. Condensed Matter Nucl. Sci.* **10** (2013) 1–14.

[59] D.J. Nagel, M. Srinivasan, Evidence from LENR Experiments for Bursts of Heat, Sound, EM Radiation and Particles and for Micro-explosions. *J. Condensed Matter Nucl. Sci.* **13** (2014) 443–454.

[60] D.F. Walls, G.J. Milburn, *Quantum Optics* (Springer, Berlin-Heidelberg, 1994), pp.73-75.

[61] P. L. Hagelstein, Constraints on energetic particles in the Fleischmann–Pons experiment, *Naturwissenschaften* **97** (2010) 345–352.
https://doi.org/10.1007/s00114-009-0644-4

[62] R. H. Dicke, Coherence in Spontaneous Radiation Processes, *Phys. Rev.* **93** (1954) 99-110.
https://doi.org/10.1103/PhysRev.93.99

[63] E. T. Jaynes, F. W. Cummings, Comparison of quantum and semiclassical radiation theories with application to the beam maser, *Proc. IEEE* **51**(1) (1963) 89-109.
doi: 10.1109/PROC.1963.1664.
[64] L. Allen, J. H. Eberly, *Optical Resonance and Two Level Atoms* (Wiley, New York, 1975) Chapter 8.
[65] P. Kálmán, T. Keszthelyi, Nuclear processes in solids: basic 2nd-order processes. arXiv:1303.1078v3
[66] P. Kálmán, T. Keszthelyi, Resonance-like nuclear processes in solids: 3rd and 4th- order processes. arXiv:1303.1262v2
[67] P. Kálmán, T. Keszthelyi, Electron assisted neutron exchange process in solid state environment. arXiv:1312.5498v2
[68] P. Kálmán, T. Keszthelyi, Cooperative internal conversion process. *J. Condensed Matter Nucl. Sci.* **25** (2017) 129-141.
[69] P. Kálmán, T. Keszthelyi, Charged particle assisted nuclear reactions in solid state environment: renaissance of low energy nuclear physics. arXiv:1502.01474v3
[70] P. Kálmán, T. Keszthelyi, Recoil assisted low energy nuclear reactions. *J. Condensed Matter Nucl. Sci.* **25** (2017) 142-158.
[71] P. Kálmán, T. Keszthelyi, Effect of impurities on nuclear fusion. arXiv:1712.05270v3
[72] C. Angulo, M. Arnould, M. Rayet, *et al.*, A compilation of charged-particle induced thermonuclear reaction rates. *Nucl. Phys. A* **656** (1999) 3-183. https://doi.org/10.1016/S0375-9474(99)00030-5
[73] H.A. Bethe, E.E. Salpeter, *Quantum Mechanics of One- and Two Electron Atoms* (Springer, Heidelberg, 1957), sec. 67.
[74] L.D. Landau, E.M. Lifshitz, *Quantum Mechanics: Non-relativistic Theory,* 3rd edn. *Course of Theoretical Physics,* Vol. 3. (Pergamon, Oxford, 1991).
[75] W.H. Louisell, *Quantum Statistical Properties of Radiation* (Wiley, New York, 1973), pp. 81-85.
[76] R.B. Firestone, V.S. Shirly, C M. Baglin, *et al.*, *Tables of Isotopes*, 8th edn. (Wiley, New York, 1996).
[77] W. Heitler, *The Quantum Theory of Radiation,* 3rd edn. (Oxford University Press, London, 1954).
[78] P.A. Mosier-Boss, S. Szpak, F.E. Gordon, *et al.*, Use of CR-39 in Pd/D co-deposition experiments. *Eur. Phys. J. Appl. Phys.* **40** (2007) 293–303. https://doi.org/10.1051/epjap:2007152
[79] P.A. Mosier-Boss, L.P. Forsley, A.S. Roussetski, *et al.*, Use of CR-39 detectors to determine the branching ratio in Pd/D co-deposition. *Current Science* **108**(4) (2015) 585-588. https://www.jstor.org/stable/24216609
[80] J.D. Bjorken, S.D. Drell, *Relativistic Quantum Mechanics* (McGraw-Hill, New York, 1964).
[81] A.B. Karabut, Y.R. Kucherov, I.B. Savvatimova, Nuclear product ratio for glow discharge in deuterium. *Phys. Lett. A* **170**(4) (1992) 265-272. https://doi.org/10.1016/0375-9601(92)90252-H
[82] J. Kasagi, H. Yuki, T. Baba, *et al.*, Low Energy Nuclear Fusion Reactions in Solids. in *8th International Conference on Cold Fusion*, Lerici (La Spezia), Italy, Italian Physical Society, Bologna, Italy (2000).
[83] P. Kálmán, T. Keszthelyi, Electron assisted dd reactions in metals. arXiv:1312.5835v3
[84] P. Kálmán, T. Keszthelyi, On low-energy nuclear reactions. arXiv:1907.05211v2
[85] M. La Cognata, S. Romano, C. Spitaleri, S. Cherubini, V. Crucillŕ, M. Gulino, L. Lamia, R.G. Pizzone, A. Tumino, R. Tribble, Changbo Fu, V.Z. Goldberg, A.M. Mukhamedzhanov, D. Schmidt, G. Tabacaru, L. Trache, B.F. Irgaziev, Astrophysical S(E) factor of the ^{15} N(p, α)^{12} C reaction at sub-Coulomb energies via the Trojan horse method. *Phys. Rev. C* **76** (2007) 065804.
https://doi.org/10.1103/PhysRevC.76.065804
[86] T.R. Fisher, W. Whaling, Reaction ^{23} Na(p, α)^{20} Ne for proton bombarding energies from 100 to 450 keV. *Phys. Rev.* **131** (1963) 1723.
https://doi.org/10.1103/PhysRev.131.1723
[87] T. Spillane, F. Raiola, C. Rolfs, D. Schürmann, F. Strieder, S. Zeng, H.-W. Becker, C. Bordeanu, L. Gialanella, M. Romano, J. Schweitzer, $^{12}C +^{12} C$ fusion reactions near the Gamow energy. *Phys. Rev. Lett.* **98** (2007) 122501.
https://doi.org/10.1103/PhysRevLett.98.122501
[88] A. Tumino, C. Spitaleri, M. La Cognata, S. Cherubini, G.L. Guardo, M. Gulino, S. Hayakawa, I. Indelicato, L. Lamia, H. Petrascu, R.G. Pizzone, S.M.R. Puglia, G.G. Rapisarda, S. Romano, M.L. Sergi, R. Spartá, L. Trache, An increase in the ^{12} C + ^{12} C fusion rate from resonances at astrophysical energies. *Nature* **557** (2018) 687-690.
https://doi.org/10.1038/s41586-018-0149-4
[89] S. Focardi, R. Habel, F. Piantelli, Anomalous heat production in Ni-H systems. *Nuovo Cimento A* **107** (1994) 163-167. https://doi.org/10.1007/BF02813080

[90] S. Focardi, V. Gabbani, V. Montalbano, *et al.*, Large excess heat production in Ni-H systems. *Nuovo Cimento A* **111**(11) (1998) 1233-1242.

[91] A. Battaglia, L. Daddi, S. Focardi, *et al.*, Neutron emission in Ni-H systems. *Nuovo Cimento* **112** (1999) 921-931. https://doi.org/10.1007/BF03035901

[92] G. J. Kroes, A. Gross, E. J. Baerends, *et al.*, Quantum theory of dissociative chemisorption on metal surfaces. *Acc. Chem. Res.* **35** (2002) 193-200. https://doi.org/10.1021/ar010104u

[93] W. Greiner, J.A. Maruhn, *Nuclear Models* (Springer, Berlin-Heidelberg, 1996).

[94] M.K. Pal, *Theory of Nuclear Structure* (Aff. East-West, New Delhi, 1982).

[95] G. Preparata, Everything You Always Wanted to know About Cold Fusion Calorimetry? in *6th International Conference on Cold Fusion: Progress in New Hydrogen Energy - ICCF- 6*, 13 - 18 Oct. 1996 - Hokkaido, Japan, ed. by M. Okamoto, pp. 136-143.

[96] J. R. Black, Electromigration-A Brief Survey and Some Recent Results, *IEEE Trans. Electron Devices*. **16** (4) (1969) 338. https://doi.org/10.1109/T-ED.1969.16754

[97] B.M. Steinetz, T.L. Benyo, V. Pines, *et al.*, Experimental Observations of Nuclear Activity in Deuterated Materials Subjected to a Low-Energy Photon Beam. NASA/TM-2017-218963 (2017), Document ID: 20170002584, available at http://www.sti.nasa.gov/.

[98] P. Kálmán, T. Keszthelyi, Photo-induced nuclear cooperation. arXiv:1904.11379.

[99] H. Bethe, R. Peiers, Quantum Theory of the Diplon. *Proc. Roy. Soc. (London) A* **148** (1935) 146-156. https://doi.org/10.1098/rspa.1935.0010

[100] H. Arenhövel, M. Sanzone, *Photodisintegration of the Deuteron: A Review of Theory and Experiment* (Springer, Wien-New York, 1991).

[101] R. Stringham, Sonofusion: Ultrasound-Activated He Production in Circulating D_2 O. *J. Condensed Matter Nucl. Sci.* **14** (2014) 79.

[102] T.N. Claytor, D.G. Tuggle, H.O. Menlove, Tritium generation and neutron measurements in Pd-Si under high deuterium gas pressure. in *The Science of Cold Fusion* Conference Porceedengs **33** Proc. 2nd Ann. Conf. on Cold Fusion ed. by T. Bressani, E. Del Guidice, G. Preparata (Italian Physical Society, Bologna, 1991), pp. 395-408.

[103] B.Y. Liaw, P.L. Tao, P. Turner, *et al.*, Elevated Temperature Excess Heat Production Using Molten-Salt Electrochemical Techniques. in *Proc. of the Special Symposium on Cold Fusion*, World Hydrogen Energy Conference **8**, Honolulu, 1990.

[104] F. David, J. Giles, Self-Polarisation of Fusion Diodes: From Excess Energy to Energy. in *Proc of the 14th Conference on Condensed Matter Nuclear Science,* ed. by D.J. Nagel, M.E. Melich (New Energy Foundation, Concord NH, 2008), p. 696.

[105] J-P. Biberian, Excess Heat Measurement in $AlLa0_3$ Doped with Deuterium. in *Proc. 5th International Conference on Cold Fusion,* ed.by S. Pons (Imra Europe, Sophia Antipolis, France, Monte-Carlo, Monaco, 1995), p. 49.

[106] G.L. Holleck, Diffusion and solubility of hydrogen in palladium and palladium–silver alloys *J. Phys. Chem.* **74** (1970) 503. https://doi.org/10.1021/j100698a005

[107] P. Colomban (Editor), *Proton conductors: Solids, membranes and gels - materials and devices* (Cambridge University Press, New York, 1992). https://doi.org/10.1002/adma.19930050923

[108] J.D. Lindl, *Inertial Confinement Fusion: The Quest for Ignition and Energy Gain Using Indirect Drive* (AIP-Press, 1998).

[109] R.S. Craxton, K.S. Anderson, T.R. Boehly, *et al.*, Direct-drive inertial confinement fusion: A review. *Phys. Plasmas* **22** (2015) 110501. https://doi.org/10.1063/1.4934714

[110] M.C.H. McKubre, F.L. Tanzella, P. Tripodi, *et al.,* The Emergence of a Coherent Explanation for Anomalies Observed in D/Pd and H/Pd System: Evidence for 4He and 3He Production. in *Proc. 8th International Conference on Cold Fusion,* ed. by F. Scaramuzzi (Italian Physical Society, Bologna, 2000), p. 3.

[111] M.C.H. McKubre, S. Crouch-Baker, A.M. Riley, *et al.*, Excess power observations in electrochemical studies of the D/Pd system; the influence of loading. in *Frontiers of Cold Fusion,* ed. by H. Ikegami (Universal Academy Press, Tokyo, 1993), pp. 5-19.

[112] K. Kunimatsu, N. Hasegawa, A. Kubota, *et al.,* Deuterium loading ratio and excess heat generation during electrolysis of heavy water by a palladium cathode in a closed cell using a partially immersed fuel cell anode. in *Frontiers of Cold Fusion,* ed. by H. Ikegami (Universal Academy Press, Tokyo, 1993), pp. 31-45.

[113] E. Storms, How basic behavior of LENR can guide a search for an explanation. *J. Condensed Matter Nucl. Sci.* **20** (2016) 100–138.

[114] E. Storms, Anomalous energy produced by PdD. *J. Condensed Matter Nucl. Sci.* **20** (2016) 81–99.

[115] S.X. Zheng, G.S. Huang, Z.M. Dong, *et al.,* Temperature Dependence of Maximum Excess Power in 3 New Experiments (Letts, Parkhomov, & Mizuno). *22nd International Conference on Condensed Matter Nuclear Science,* Assisi, Italy, 2019.

[116] M. Srinivasan, G. Miley, E. Storms, Low Energy Nuclear Reactions: Transmutations, in *Nuclear Energy Encyclopedia: Science, Technology, and Applications,* ed. by S.B. Krivit, J.H. Lehr, T.B. Kingery (John Wiley & Sons Online Library, New Jersey, 2011), Part VI. Ch. **43** pp. 481-502.

[117] G. Levi, E. Foschi, B. Höistad, *et al.*, Observation of abundant heat production from a reactor device and of isotopic changes in the fuel. http://www.sifferkoll.se/sifferkoll/wp-content/uploads/2014/10/LuganoReportSubmit.pdf

[118] G.H. Miley, J.A. Patterson, Nuclear Transmutations in Thin-film Nickel Coatings undergoing Electrolysis. *J. New Energy* **1** (1996) 5-30.

[119] C.P. Berlinguette, Y.M. Chiang, J.N. Munday, *et al.*, Revisiting the cold case of cold fusion. *Nature* **570** (2019) 45-51. https://doi.org/10.1038/s41586-019-1256-6

[120] SPAWAR Hot Spot Video. https://www.youtube.com/watch?v=OUVmOQXBS68

[121] S. Szpak, P.A. Mosier-Boss, F.E. Gordon, Experimental evidence for LENR in a Polarized Pd/D Lattice. *National Defense Industry Association Conference*, Washington DC, 2006. http://lenr-canr.org/wordpress/?page_id=1081

[122] D.J. Nagel, M. Srinivasan, Evidence from LENR Experiments for Bursts of Heat, Sound, EM Radiation and Particles and for Micro-explosions. J. Condensed Matter Nucl. Sci. **13** (2014) 443–454.

[123] D.J. Nagel, A.E. Moser, High Energy Density and Power Density Events in Lattice-enabled Nuclear Reaction Experiments and Generators. J. Condensed Matter Nucl. Sci. **19**, 219–229 (2016).

[124] M. Srinivasan, Hot Spots, Chain Events and Micro-Nuclear Explosions, in *15th Int. Conf. on Condensed Matter Nuclear Science*, Rome, Italy, Oct. 5-9, 2009, Proc. ICCF-15, ed. by V. Violante, F. Sarto, pp. 240-245.

[125] H. Kozima, W-S. Zhang and J. Dash, Precision measurement of excess energy in electrolytic system Pd/D/H2SO4 and inverse power distribution of energy pulses vs. excess energy. *Proc. of the 13th Int. Conf. on Condensed Matter Nuclear Science,* MATI Moscow, 2008, pp. 348–358.

[126] F. Raiola, P. Migliardi, G. Gyürky, *et al.*, Enhanced electron screening in $d(d,p)t$ for deuterated Ta. *Eur. Phys. J. A - Hadrons and Nuclei* **13** (2002) 377–382. https://doi.org/10.1007/s10050-002-8766-5

[127] F. Raiola, P. Migliardi, L. Gang, *et al.*, Electron screening in $d(d,p)t$ for deuterated metals and the periodic table. *Phys. Lett. B* **547** (2002) 193-199. https://doi.org/10.1016/S0370-2693(02)02774-0

[128] C. Bonomo, G. Fiorentini, Z. Fülöp, *et al.*, Enhanced electron screening in $d(d,p)t$ for deuterated metals: a possible classical explanation. *Nucl. Phys. A* **719** (2003) C37-C42. https://doi.org/10.1016/S0375-9474(03)00955-2

[129] J. Kasagi, H. Yuki, T. Baba, *et al.*, Strongly Enhanced DD Fusion Reaction in Metals Observed for keV D^+ Bombardment. *J. Phys. Soc. Jpn.* **71** (2002) 2881-2885. https://doi.org/10.1143/JPSJ.71.2881

[130] K. Czerski, A. Huke, A. Biller, *et al.*, Enhancement of the electron screening effect for d + d fusion reactions in metallic environments. *Europhys. Lett.* **54** (2001) 449. https://doi.org/10.1209/epl/i2001-00265-7

[131] K. Czerski, A. Huke, P. Heide, *et al.*, Solid-state effects in d+d fusion reactions. *Nucl. Instr. and Meth. in Phys. Res. B* **193** (2002) 183-187. https://doi.org/10.1016/S0168-583X(02)00747-4

[132] A. Huke, K. Czerski, P. Heidea, Experimental techniques for the investigation of the electron screening effect for d+d fusion reactions in metallic environments. *Nucl. Phys. A* **719** (2003) C279-C282. https://doi.org/10.1016/S0375-9474(03)00932-1

[133] P. Kálmán, T. Keszthelyi, Forbidden nuclear reactions in astrophysics. https://www.researchgate.net/publication/344679769_Forbidden_nuclear_reactions_in_astrophysics

[134] C. Iliadis, *Nuclear Physics of Stars* (Wiley-VCH, Weinheim, 2015) p. 146, (3.26).

[135] H.E. Bond, E.P. Nelan, D.A. VandenBerg, G.H. Schaefer, D. Harmer, HD 140283: A Star in the Solar Neighborhood that Formed Shortly after the Big Bang. *Astrophys. J.* **765** (2013) L12. https://doi.org/10.1088/2041-8205/765/1/L12